

University of New Mexico
UNM Digital Repository

Physics & Astronomy ETDs

Electronic Theses and Dissertations

8-27-2009

Applications of statistical mechanics and nonlinear science to ecological phenomena

Luis Felipe Gonzalez-Palacio

Follow this and additional works at: https://digitalrepository.unm.edu/phyc_etds

Recommended Citation

Gonzalez-Palacio, Luis Felipe. "Applications of statistical mechanics and nonlinear science to ecological phenomena." (2009).
https://digitalrepository.unm.edu/phyc_etds/17

This Thesis is brought to you for free and open access by the Electronic Theses and Dissertations at UNM Digital Repository. It has been accepted for inclusion in Physics & Astronomy ETDs by an authorized administrator of UNM Digital Repository. For more information, please contact disc@unm.edu.

Luis Felipe Gonzalez-Palacio

Candidate

Physics & Astronomy

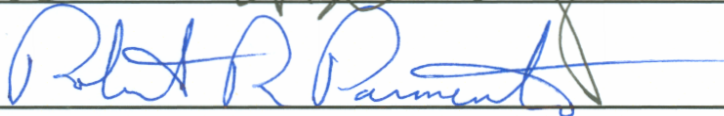
Department

This thesis is approved, and it is acceptable in quality and form for publication:

Approved by the Thesis Committee:



,Chairperson



Applications of Statistical Mechanics and Nonlinear Science to Ecological Phenomena

by

Luis Felipe Gonzalez-Palacio

B.S., Civil Engineering, Escuela Colombiana de Ingenieria, 2005

THESIS

Submitted in Partial Fulfillment of the
Requirements for the Degree of

Master of Science
Physics

The University of New Mexico

Albuquerque, New Mexico

July, 2009

©2009, Luis Felipe Gonzalez-Palacio

Dedication

To my parents.

To my family.

To D.

Acknowledgments

I want to thank my parents and family for their unconditional love and support throughout my entire life. This new achievement would not have been possible without you. I also want to thank Prof. Vasudev Kenkre, my friend, mentor, and advisor, for believing in me and inviting me to be part of his group for the past three years: thank you for giving me the unique opportunity to study very exciting physics and for encouraging me to be creative and to see things from a different perspective. Also, I would like to thank Prof. Bernardo Lievano for sharing with me the excitement of physics, and Dr. Michael Raghieb for introducing me to Prof. Kenkre and to the Consortium of the Americas for Interdisciplinary Science.

I want to thank Dr. Bob Parmenter for providing me with the invaluable field data, the analysis of which forms the backbone of this thesis, as well as vast amounts of biological insight and intuition. Also, thanks for agreeing to be part of my thesis committee, along with Prof. David Dunlap, one of the best instructors in our department. I want to acknowledge Dr. Marcelo Kuperman for his support regarding computational aspects of the data analysis. I would also like to gratefully acknowledge the support of the Department of Physics and Astronomy at UNM, including Dr. Kathryn Dimiduk and Prof. Bernd Bassalleck. The Consortium of the Americas for Interdisciplinary Science provided invaluable support throughout my stay here in Albuquerque, thus I would like to thank Lela Castillo, Assistant to the Director of the Consortium, and Adriana Recalde, who occupied this position before Lela.

I want to thank fellow students Ben Baragiola, Mukesh Tiwari, Ziya Kalay, Sabrina Araujo, Elizabeth Merritt, Dave MacInnis, Debbie Cox, Ali Masoud, and Xiaomo Ying. Thanks for all the studying, discussions, and great conversations regarding physics, but above all, thanks for making my life so much better.

And last but not least, I would like to thank the Gentilini family, particularly Dywane, Pam, Marge, and Fargo for making my stay in Albuquerque so much better than it would have been had I not met you.

Applications of Statistical Mechanics and Nonlinear Science to Ecological Phenomena

by

Luis Felipe Gonzalez-Palacio

ABSTRACT OF THESIS

Submitted in Partial Fulfillment of the
Requirements for the Degree of

Master of Science
Physics

The University of New Mexico

Albuquerque, New Mexico

July, 2009

Applications of Statistical Mechanics and Nonlinear Science to Ecological Phenomena

by

Luis Felipe Gonzalez-Palacio

B.S., Civil Engineering, Escuela Colombiana de Ingenieria, 2005

M.S., Physics, University of New Mexico, 2009

Abstract

The application of techniques widely used in physics to explain biological phenomena has become a very successful endeavor in the past few decades. Such techniques include, but are not limited to, kinetic equations and nonlinear dynamics.

We present an overview of some current topics of interest in ecology that use such techniques to explain and predict a wide array of phenomena. Several successful models are reviewed.

We present the results of our analyses of two datasets of repeated sessions of mark-recaptures of the deer mouse, *Peromyscus maniculatus* (Rodentia: Muridae), the host and reservoir of Sin Nombre Virus (Bunyaviridae: Hantavirus). The first dataset corresponds to a three-year period of mark-recaptures in the Valles Caldera National Preserve, New Mexico. The second one corresponds to a four-year period

of mark-recaptures in the Wyoming grassland. We study the displacements of the recaptured rodents from a web distribution of traps on the landscape (New Mexico), and a square grid (Wyoming). From the displacements we extract the diffusion constant of the motion of the rodents. In New Mexico, the short-time behavior (1 day) shows the motion to be approximately diffusive and the diffusion constant to be $320 \pm 40 \text{ m}^2/\text{day}$. In Wyoming, the average diffusion constant for the deer mice was $105 \pm 10 \text{ m}^2/\text{day}$. The long-time behavior is capable, in principle, of providing an estimation of the extent of the rodent home ranges. However, the datasets analyzed were not sufficiently detailed to yield a value for the home ranges, and the focus of the thesis is on the diffusion constants rather than on the home ranges.

Contents

List of Figures	xi
List of Tables	xiv
1 Introduction	1
2 A Survey of Some Current Topics in Ecology and Epidemics	4
2.1 Overview	4
2.2 Theoretical Background	5
2.2.1 Some Statistical Mechanics	5
2.2.2 Some Nonlinear Dynamics	11
2.3 Nonspatial Models: Malthus, Verhulst, and the Allee Effect	16
2.4 Spatial Models: Reaction-Diffusion and Wavefronts	17
2.4.1 An Experimental Argument	18
2.4.2 A Theoretical Argument	18
2.4.3 The SI model for epidemics	20

Contents

2.4.4	The SIR model for epidemics	23
2.5	Spatial Models: Reaction-Diffusion and The Existence of a Minimal Domain Size	27
2.5.1	Boundary Conditions	28
2.5.2	The Eigenvalue Approach	30
2.5.3	The Energy Method Revisited	34
2.6	Spatial Models: Reaction-Diffusion and Patterns	36
3	Diffusion Constants of Rodents in New Mexico and Wyoming	41
3.1	Overview	41
3.2	Recapture of animals and displacement measurement	42
3.3	Renormalization of the measurements and estimation of the diffusion constants	48
3.4	Movement Parameters	50
3.4.1	Results: Wyoming	50
3.4.2	Results: New Mexico	58
4	Conclusions	59
	References	62

List of Figures

2.1	Micro, meso, and macroscopic descriptions in physics.	5
2.2	General structure of an infinite chain.	6
2.3	Mean square displacement vs. time, assuming that $\langle m^2 \rangle_0 = 0$. This plot is sometimes called an Einstein result.	8
2.4	General structure of an infinite chain, with distance a between chain sites.	9
2.5	General form of a logistic system, for $a > 0$	14
2.6	General form of a logistic system, for $a = 0$	14
2.7	General form of a logistic system, for $a < 0$	15
2.8	Transcritical bifurcation.	15
2.9	The length of the patch, l , versus the maximum density, u_{max} , for the logistic case. After Cantrell and Cosner [1].	36
2.10	Sketch of a hypercycle with 6 self-replicating molecular species and one parasite species that gets help replicating from species 2 but won't help anyone but itself to replicate. Based on figures from Dieckmann, Law, and Metz [2].	39

List of Figures

2.11	Reaction-diffusion spiral for five species. The color at each point represents the species with the highest concentration at that given point. Copyright Wikimedia Commons.	40
3.1	Schematic arrangement of each of the 9 trapping webs used to obtain the New Mexico dataset. Each dot represents a Sherman trap. There is only one trap at the center as opposed to four traps in II. The four inner circles have radii increasing in 5 m intervals, while the rest are separated by 10 m. There are 145 traps per web. [3,4].	44
3.2	Schematic arrangement of each of the 3 square trapping grids used to obtain the Wyoming dataset. Each dot represents a Sherman trap. Each grid has 225 traps, with 10 meters between traps in the two spatial directions. Each grid has a side of length 140 m, with 100 m between each grid.	45
3.3	Observed distribution $q(r)$ of displacements r at several time scales, compared with the distribution $w(r)$ of distances in the web, for New Mexico.	46
3.4	Distribution of East-West and North-South distances in the web trapping configuration (New Mexico). The diameter of the grid is 200 m.	47
3.5	Distribution of East-West and North-South distances in the square grid trapping configuration (Wyoming). The side of the grid is 140 m.	47
3.6	Probability distribution of observed displacements for <i>P. maniculatus</i> in the East-West direction for the 1 day time-scale (New Mexico).	48
3.7	Renormalized probability distribution of actual displacements that characterizes the movement of <i>P. maniculatus</i> in the East-West direction at 1 day (New Mexico). The continuous line shows the least-squares Gaussian fit of the distribution ($\chi^2 = 1.0 \times 10^{-5}$).	49

List of Figures

3.8	Diffusion constant vs. number of individuals for the total, adult, and juvenile populations (Wyoming).	53
3.9	Number of individuals vs. time for the total, adult, and juvenile populations (Wyoming).	53
3.10	Diffusion constant vs. time for the total, adult, and juvenile populations (Wyoming).	54
3.11	Diffusion constant vs. the number of individuals for the total, male, and female populations (Wyoming).	55
3.12	Number of individuals vs. time for the total, male, and female populations (Wyoming).	55
3.13	Diffusion constant vs. time for the total, male, and female populations (Wyoming).	56
3.14	Diffusion constant vs. the number of individuals for adult males, adult females, and total adult populations (Wyoming).	56
3.15	Number of individuals vs. time for adult males, adult females, and total adult populations (Wyoming).	57
3.16	Diffusion constant vs. time for adult males, adult females, and total adult populations (Wyoming).	57
3.17	Mean square displacement in the two spatial directions as a function of time for <i>P. maniculatus</i> (New Mexico). The initial slope of each curve is $2D$, where D is the diffusion coefficient.	58

List of Tables

3.1	Diffusion constants in the two spatial directions at the short time scale (1 day) for Wyoming.	52
3.2	Diffusion constants in the two spatial directions at the short time scale (1 day) for New Mexico.	58

Chapter 1

Introduction

It is a great time to be a physicist. Our discipline has proven time and again that it is capable of solving or of helping solve daunting questions about the world. In this spirit, collaboration with other sciences, both natural and social, becomes viable and indeed very rewarding. With this in mind, for the purposes of this thesis, physics has become a driving force behind aspects of biology, more specifically, ecology.

The research group to which the author belongs has been immersed in very exciting research within the field of mathematical biology for quite some time now, studying aspects of the Hantavirus, the West-Nile virus, and the Bubonic Plague, among other topics [5–8]. As the author was looking for a project for his thesis last year, Prof. Kenkre, his thesis advisor, invited Dr. Bob Parmenter, Research Professor at UNM’s Department of Biology and Chief Scientist at Valles Caldera National Preserve (New Mexico) for a talk last summer, and they both got the author very excited with the topic of epidemics. There was an opportunity to analyze *real* field data that had been collected primarily to estimate population densities of rodents. The author undertook to find diffusion constants for the movement of rodents in the field, thus the results of the analysis of the data form the backbone of the present

Chapter 1. Introduction

thesis (see Chapter 3). As will be explained in Chapter 2, the diffusion constant is one of the key parameters in the study of epidemics via reaction-diffusion equations. It measures how, on average, a given population (of rodents, for example) diffuses or moves in space, and is given in units of m^2/day throughout Chapter 3.

Chapter 2 starts with a compendium of a certain collection of topics in statistical mechanics and nonlinear science that are relevant to ecology. We also present an overview of some related topics in modern ecology. We describe the importance of patterns in ecology and how they have been successfully predicted in our group via the Abramson-Kenkre model [5], as well as modifications to that model [8,9]. We look at the need for reaction-diffusion equations in mathematical biology and ecology [10], and look at ways to apply these equations in order to describe and predict the behavior of several epidemics [5,6,8]. Other related concepts such as home ranges of the moving animals are discussed here as well.

In Chapter 3 we present the results of our analyses of two datasets of repeated sessions of mark-recaptures of the deer mouse, *Peromyscus maniculatus* (Rodentia: Muridae), the host and reservoir of Sin Nombre Virus (Bunyaviridae: Hantavirus). The first dataset corresponds to a three-year period in the Valles Caldera National Preserve, New Mexico. The second corresponds to a four-year period of mark-recaptures in the Wyoming grassland. We study the displacements of the recaptured rodents from two different distributions of traps on the landscape: web (New Mexico) and square grid (Wyoming). The results of both datasets are compared and contrasted, and physical quantities are extracted, within the limitations of the data available. Most of the discussion is focused on the diffusion of the rodents on the landscape, but the important concept of home range is also discussed, although with less emphasis than the main focus of the investigation, the diffusion constants.

Chapter 4 presents the concluding remarks of the present thesis. Conclusions

Chapter 1. Introduction

are drawn mainly from the analysis of the datasets presented in Chapter 3, in the context of the review of topics presented in Chapter 2.

Chapter 2

A Survey of Some Current Topics in Ecology and Epidemics

2.1 Overview

There is a vast amount of available literature regarding past and present research in the fields of ecology and epidemics. In the present chapter we introduce the basic concepts of statistical mechanics and nonlinear science used in and around this thesis to tackle ecological problems from a mathematical perspective [1, 2, 10]. We introduce the essential concepts of diffusion and reaction-diffusion equations. Within ecology [1, 2, 10], the latter are used to model wavefront propagation (those that travel without changing their shape), the existence of a minimal spatial region or domain that can support positive species density profiles [1], and pattern formation [1, 2]. These three cases will be described in detail later in the present chapter.

2.2 Theoretical Background

2.2.1 Some Statistical Mechanics

When we use Newton's, Hamilton's, Schrodinger's, and Liouville's equations and we reverse time, no difference of a qualitative nature occurs in the evolution. Any finite system can always come back arbitrarily close to any previous state it occupied in the past. This fundamental principle was enunciated by Poincaré for classical systems. These are called Poincaré cycles (recurrences) and they are related to the size of the system. In quantum systems, it was proven by Bocchieri and Loinger, and it all points at the question of the direction of time, because it is clear that things die, they *decay*, instead of just oscillating in time. Now comes one of the big questions in all of physics: how do *reversible* equations of motion at the microscopic level result in *irreversible* phenomena at the macroscopic level? (see Fig. 2.1). In other words, how do oscillations end up in decay?

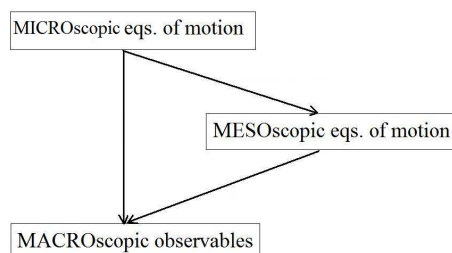


Figure 2.1: Micro, meso, and macroscopic descriptions in physics.

At the mesoscopic level, decay is built into the equations. Thus, it is natural to

ask the question, what kind of equations of motion live in the mesoscopic level? The answer is the Master equation, the Chapman-Kolmogorov equation (random walk), the Boltzmann equation, etc.

Let us suppose, for simplicity, that we have two sites, left (L) and right (R). The probability of being at site L at any given time is given by $P_L(t)$ and the probability of being at site R at any given time is given by $P_R(t)$. $P_L(t) + P_R(t) = 1$. The index m can take either L or R :

$$\frac{dP_L(t)}{dt} = FP_R(t) - FP_L(t), \quad (2.1)$$

$$\frac{dP_R(t)}{dt} = FP_L(t) - FP_R(t), \quad (2.2)$$

and the general expression for the Master equation is given by

$$\frac{dP_m(t)}{dt} = \sum_n F_{mn}P_n(t) - F_{nm}P_m(t). \quad (2.3)$$

This is a simple form, called the *gain-loss form*, of the Master equation [11]. It is the evolution equation for the probabilities of occupation of the states by the system, and is always written as a linear equation.

Now let us picture a random walker on an infinite chain,

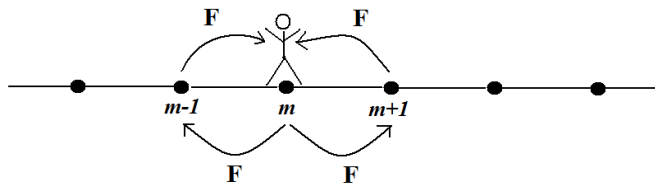


Figure 2.2: General structure of an infinite chain.

where F are the transition rates from one site to another (taken to be the same in this case), the sites being labeled by $m, m - 1, m + 1$, etc. Let us write down the

Master equation for the chain in Fig. 2.2,

$$\frac{dP_m}{dt} = F(P_{m+1} + P_{m-1}) - F(P_m + P_m), \quad (2.4)$$

for a translationally invariant system, that is, one in which any site is equivalent to any other site. We can rewrite this expression as

$$\frac{dP_m}{dt} = F(P_{m+1} + P_{m-1} - 2P_m), \quad (2.5)$$

and we ask the question, where is this random walker? We look at the *mean displacement*, given by

$$\langle m \rangle = \sum_{m=-\infty}^{\infty} mP_m, \quad (2.6)$$

and find that it vanishes for symmetrical reasons. Therefore we look at the *mean square displacement*:

$$\langle m^2 \rangle = \sum_{m=-\infty}^{\infty} m^2 P_m. \quad (2.7)$$

Now let us multiply both sides of Eq. 2.5 by m^2 and sum. Then,

$$\frac{d\langle m^2 \rangle}{dt} = F \sum_{m=-\infty}^{\infty} m^2 P_{m+1} + F \sum_{m=-\infty}^{\infty} m^2 P_{m-1} - 2F \langle m^2 \rangle. \quad (2.8)$$

After some algebra we arrive at the main result,

$$\frac{d\langle m^2 \rangle}{dt} = 2F. \quad (2.9)$$

The solution for the dimensionless mean square displacement is thus

$$\langle m^2 \rangle = \langle m^2 \rangle_0 + 2Ft. \quad (2.10)$$

The mean square displacement increases linearly with time (see Fig. 2.3).

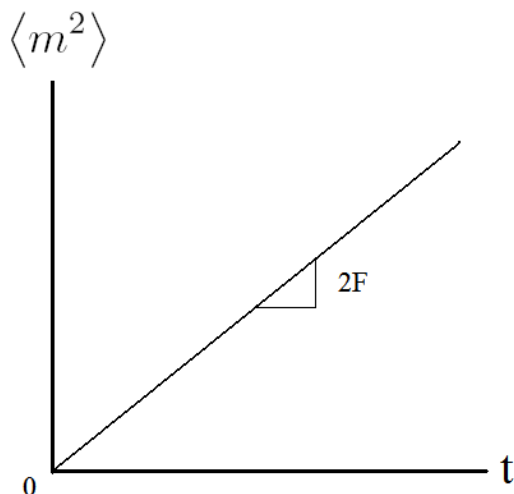


Figure 2.3: Mean square displacement vs. time, assuming that $\langle m^2 \rangle_0 = 0$. This plot is sometimes called an Einstein result.

The Continuum Limit

Let us connect the Master equation with the diffusion equation. Let us assume that our random walker has a hopping distance a , called the *lattice constant* in solid state physics (see Fig. 2.4).

The dimensioned mean square displacement (with units of the square of length) is given by

$$a^2 \langle m^2 \rangle = \langle x^2 \rangle, \quad (2.11)$$

$$\langle x^2 \rangle = \langle x^2 \rangle_0 + (2Fa^2)t, \quad (2.12)$$

and we can say that $\frac{dP_m}{dt}$ is a difference of differences:

$$\frac{dP_m}{dt} = a^2 F \left[\frac{(P_{m+1} - P_m)}{a} - \frac{(P_m - P_{m-1})}{a} \right]. \quad (2.13)$$

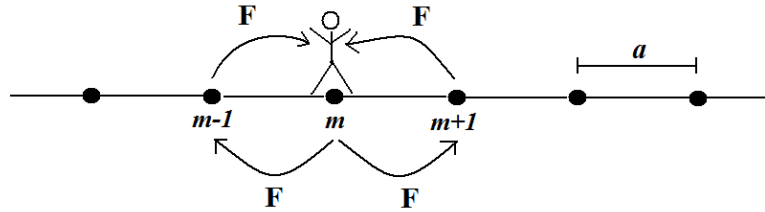


Figure 2.4: General structure of an infinite chain, with distance a between chain sites.

In the continuum limit $a \rightarrow 0$, at the same time with $F \rightarrow \infty$, and $Fa^2 \rightarrow D$, we get

$$\frac{\partial P(x, t)}{\partial t} = D \frac{\partial^2}{\partial x^2} P(x, t), \quad (2.14)$$

called the diffusion, heat, or Fourier equation, where D is the diffusion constant. The parameter D has a special role in the modeling of epidemics (see Chapter 3), thus it will be thoroughly discussed there. The mean square displacement is given by

$$\langle x^2 \rangle = \int_{-\infty}^{\infty} x^2 P(x, t) dt = 2(Fa^2)t = 2Dt. \quad (2.15)$$

We can solve the diffusion equation for arbitrarily initial conditions by using Fourier transforms. We start with the initial condition $P(x, 0) = \delta(x)$, and we solve this for all initial conditions. Since Eq. 2.14 is a linear equation, we can use superposition to solve it.

Solving the Discrete Case

Let us solve the discrete case of the diffusion equation for arbitrary initial conditions:

$$\frac{dP_m(t)}{dt} = F(P_{m+1} + P_{m-1} - 2P_m). \quad (2.16)$$

Let us use the discrete Fourier Transform,

$$P^k = \sum_{m=-\infty}^{\infty} P_m e^{ikm}. \quad (2.17)$$

Chapter 2. A Survey of Some Current Topics in Ecology and Epidemics

After multiplying by e^{ikm} and summing over all m , Eq. 2.16 turns into

$$\frac{dP^k}{dt} + 4 \sin^2(k/2)FP^k = 0, \quad (2.18)$$

whose solution is given by

$$P^k(t) = P^k(0)e^{-4Ft \sin^2(k/2)}, \quad (2.19)$$

and let us go back to m -space in order to have a complete solution after inverting the transform. Let us consider the simplest case, $P_m(0) = \delta_{m,0}$:

$$P^k(0) = \sum_{m=-\infty}^{\infty} P_m(0)e^{ikm} = 1, \quad (2.20)$$

$$P^k(t) = e^{-4Ft \sin^2(k/2)} = e^{-2Ft(1-\cos k)}. \quad (2.21)$$

Now let us turn back to m , which takes integer values from $-\infty$ to ∞ , while k takes continuous values. The solution for $P_m(t)$ when $P_m(0) = \delta_{m,0}$ is

$$P_m(t) = I_m(2Ft)e^{-2Ft}, \quad P_m(0) = \delta_{m,0}, \quad (2.22)$$

where we have the Bessel function $I_m(2Ft)$. In general we have

$$P_m(t) = \sum_{n=-\infty}^{\infty} \psi_{m-n}(t)P_n(0), \quad (2.23)$$

where the so-called propagator $\psi_{m-n}(t)$ is the solution for the delta function localized condition mentioned above.

Solving the Continuum Case

Let us start with Eq. 2.14,

$$\frac{\partial P(x,t)}{\partial t} = D \frac{\partial^2 P(x,t)}{\partial x^2}. \quad (2.24)$$

We have solved the discrete case with Bessel functions, now let us solve the continuum case. Let us use Fourier Transforms:

$$\hat{P}(k, t) = \int_{-\infty}^{\infty} P(x, t) e^{ikx} dx \rightarrow P(x, t) = \frac{1}{2\pi} \int_{-\pi}^{\pi} \hat{P}(k, t) e^{-ikx} dk, \quad (2.25)$$

$$\frac{d}{dt} \hat{P}(k, t) = -Dk^2 \hat{P}(k, t), \quad \hat{P}(k, t) = \hat{P}(k, 0) e^{-Dk^2 t}. \quad (2.26)$$

The Fourier inverse is

$$P(x, t) = \int_{-\infty}^{\infty} \Psi(x - x', t) P(x', 0) dx', \quad (2.27)$$

where $P(x', 0)$ is an initial condition and $\Psi(x - x', t)$ is the propagator, which is the Fourier-inverse of $e^{-Dk^2 t}$. For the discrete case we have $e^{-2Ft(1-\cos k)}$, where k is dimensionless, and for the continuum case we have $e^{-Dk^2 t}$, where k has units of 1/distance and we will call it q . Starting from the discrete case we have, as $k \rightarrow 0$, $q = k/a$, and $Fa^2 \frac{k^2}{a^2} t \rightarrow Dq^2 t$, and the propagator is given by

$$\Psi(x, t) = \frac{1}{2\pi} \int_{-\infty}^{\infty} e^{-Dq^2 t} e^{-iqx} dq \Rightarrow \frac{1}{\sqrt{4\pi Dt}} e^{-\frac{x^2}{4Dt}}. \quad (2.28)$$

This expression will be of paramount importance in Chapter 3 when we study the probability distributions of mice diffusing on the terrain. At different time scales, e.g., 1 day, 2 days, 30 days, etc., from the data we will find a propagator that approximates this shape, thus we will fit our distributions to resemble a Gaussian shape in order to compute the mean square displacement as needed.

2.2.2 Some Nonlinear Dynamics

The last thirty or forty years have seen tremendous advances in the theory of nonlinear science, which in turn have pushed forward the field of reaction-diffusion equations [1, 2, 10, 12]. These equations occupy a central role in the modeling of epidemics

Chapter 2. A Survey of Some Current Topics in Ecology and Epidemics

as will be seen throughout this thesis. For this reason we will spend some time studying some basic aspects of nonlinear dynamics.

Some examples of linear systems are

$$\frac{dy}{dt} + \alpha y = 0, \quad (2.29)$$

$$\frac{d^2y}{dt^2} + \omega^2 y = 0, \quad (2.30)$$

$$-\frac{\hbar^2}{2m} \frac{\partial^2 \psi(x,t)}{\partial x^2} + V(x)\psi(x) = i\hbar \frac{\partial \psi(x,t)}{\partial t}. \quad (2.31)$$

Some examples of nonlinear systems are

$$\frac{dy}{dt} + \beta y^2 = 0, \quad (2.32)$$

$$\frac{d^2y}{dt^2} + \sin y = 0, \quad (2.33)$$

$$\frac{d^2y}{dt^2} + \alpha \left(\frac{dy}{dt} \right)^{17} + \omega^2 y = 0. \quad (2.34)$$

Nonlinear systems exhibit disappearance of superposition of initial conditions and also superposition of responses corresponding to given stimuli. To explain the former, let us take Eq. 2.29:

$$\frac{dy}{dt} + \alpha y = 0, \quad (2.35)$$

whose solution, for the initial condition $y(0)$, is well-known:

$$y(t) = y(0)e^{-\alpha t}. \quad (2.36)$$

If now we have the initial condition $y_1(0) + y_2(0)$, we get the solution

$$y(t) = [y_1(0) + y_2(0)] e^{-\alpha t}, \quad (2.37)$$

Chapter 2. A Survey of Some Current Topics in Ecology and Epidemics

so the propagator or Green function, $e^{-\alpha t}$, stays the same, meaning we have superposition of initial conditions. For a nonlinear expression such as Eq. 2.32,

$$\frac{dy}{dt} + \beta y^2 = 0, \tag{2.38}$$

for an initial condition $y(0)$, the solution is

$$y(t) = y(0) \left(\frac{1}{1 + \beta t y(0)} \right), \tag{2.39}$$

and it is clear that the Green function changes compared to the linear case (it becomes dependent on the initial condition).

In the context of the superposition of responses for given stimuli, let us take a linear equation plus a constant,

$$\frac{dy}{dt} = -\alpha y + S, \tag{2.40}$$

where S is called the stimulus, and if we take the limit as $t \rightarrow \infty$, we get

$$\text{Lim}_{t \rightarrow \infty} y(t) = \frac{1}{\alpha} S. \tag{2.41}$$

If we had S_1, S_2 , we would get $\frac{1}{\alpha} (S_1 + S_2)$. This does not happen in nonlinear systems.

There are very interesting aspects regarding nonlinear systems. We encounter a richness of new phenomena, including:

- Abrupt transitions
- Thresholds
- Chaos (sensitivity to initial conditions)
- Bifurcations

Chapter 2. A Survey of Some Current Topics in Ecology and Epidemics

Let us focus, for the purpose of the present thesis, on bifurcations, and for this let us use a classic example of a nonlinear system [10, 12],

$$\frac{dy}{dt} = ay - by^2, \tag{2.42}$$

also known as the *logistic equation*, that describes, for instance, the population density of animals, growing by birth (linear term) and dying by competition (bilinear term) (Fig. 2.5).

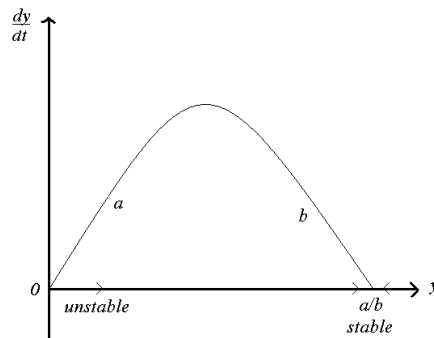


Figure 2.5: General form of a logistic system, for $a > 0$.

If $a = 0$, we get Fig. 2.6.

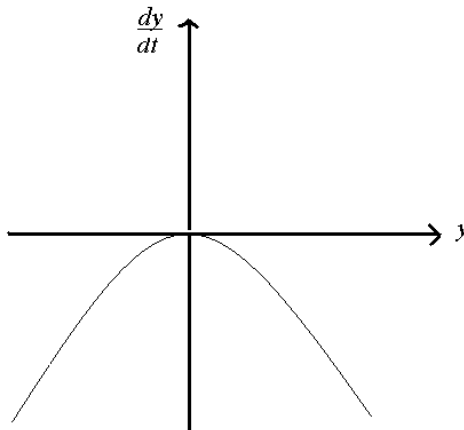


Figure 2.6: General form of a logistic system, for $a = 0$.

If $a < 0$, we get Fig. 2.7.

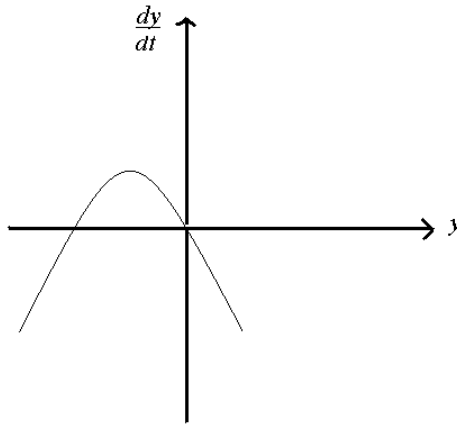


Figure 2.7: General form of a logistic system, for $a < 0$.

We are interested in observing the change in the stability of the fixed points as we change a . We do this using a bifurcation diagram (see Fig. 2.8). This is called a *transcritical bifurcation*, and is a key feature of the AK model for the spread of the Hantavirus discussed later in this chapter.

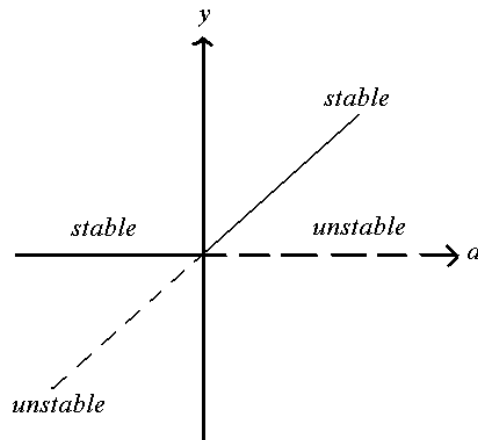


Figure 2.8: Transcritical bifurcation.

2.3 Nonspatial Models: Malthus, Verhulst, and the Allee Effect

For many years investigators have tried to explain and predict epidemics using whatever tools, mathematical or otherwise, were available at the time [10]. Malthus (1798) [1, 10] has been widely credited with attempting to model population dynamics for the first time. His model for population growth is a density-independent (r not dependent on u) model or a linear growth model [1, 12], given by

$$\frac{du(t)}{dt} = r(t)u(t), \quad (2.43)$$

where $u(t)$ is the density of some population at time t , and $r(t)$ is the birth rate of the population. If the growth rate is constant, the solution to this equation is given by

$$u(t) = u(0)e^{rt}, \quad (2.44)$$

meaning we have either exponential growth or decay for the population as a function of time, depending on the sign of r .

Another important model in the spread of epidemics is the one attributed to Verhulst (1838) [1, 10, 12]: now the growth rate is affected by the population density, and using the standard form ubiquitous in the biology literature [1] we write the expression as

$$\frac{du(t)}{dt} = r \left(1 - \frac{u(t)}{K} \right) u(t), \quad (2.45)$$

where r is called the *intrinsic* growth rate of the population [1, 10], and K is called the *carrying capacity* (more on this parameter will be discussed later). This is called the *logistic equation* and is ubiquitous in the ecology and epidemics literature. Using the language of nonlinear dynamics [10, 12], we can say positive solutions approach

the equilibrium point or fixed point $u(t) = K$ in a *monotonic* fashion, and it is a stable fixed point; the point $u(t) = 0$ is unstable. There is yet another important case as we go from linear (Malthusian) to quadratic (Verhulst or logistic) to cubic. The latter is called the *Allee effect* [1, 10, 12] and says that if the density falls below a certain critical value, the population will eventually die. Kenkre and collaborators have investigated the consequences of introducing Allee effects in reaction diffusion systems [13–15]. An expression that models this behavior is given by

$$\frac{du(t)}{dt} = r(u(t) - \alpha)(K - u(t))u(t), \quad (2.46)$$

where $r > 0$ and $0 < \alpha < K$. Any solutions between $u(t) = 0$ and $u(t) = \alpha$ will go to $u(t) = 0$, but solutions that start at $K > u(t) > \alpha$ will go to $u(t) = K$ monotonically ($u(t) = 0, K$ are stable and $u(t) = \alpha$ is unstable).

In order to study the *spatial* component of ecology we have to add something to our equations that describes *motion in space*, and that is when *diffusion* comes to mind. Let us take a look at the very important concepts of *diffusion* and *reaction-diffusion*.

2.4 Spatial Models: Reaction-Diffusion and Wavefronts

In this section we review the first of three main applications [1, 2] of reaction-diffusion equations in the context of spatial ecology: the problem of propagating wavefronts.

2.4.1 An Experimental Argument

Many phenomena in biology deal with the appearance of a traveling wave (mechanical deformation or chemical concentration) [6, 10]. We may use the diffusion equation

$$\frac{\partial u(x, t)}{\partial t} = D \frac{\partial^2 u(x, t)}{\partial x^2}, \quad (2.47)$$

to study the behavior of the wave-fronts, but if we take a length of the order of 1 mm, and use values of D for say, developing embryos ($10^{-9} - 10^{-11} \text{cm}^2/\text{sec}$), we would get times of the order of $10^7 - 10^9 \text{sec}$ which are extremely large for an early embryonic process [10]. Thus, from the experiments we see the need for reaction-diffusion equations of the form

$$\frac{\partial u}{\partial t} = f(u) + D \frac{\partial^2 u}{\partial x^2}, \quad (2.48)$$

where $f(u)$ represents the kinetics and D is the diffusion constant.

2.4.2 A Theoretical Argument

In order to model wavefront propagation, if we have a solution of the form

$$u(x, t) = u(x - ct) = u(z), \quad z = x - ct, \quad (2.49)$$

$$D \frac{d^2 u}{dz^2} + c \frac{du}{dz} = 0 \Rightarrow u(z) = A + B e^{-cz/D} \quad (2.50)$$

and since u has to be bounded for all z , then B must be zero because the exponential becomes unbounded as $z \rightarrow -\infty$. $u(z) = A$ is *not* a wave solution, so we can see that pure diffusion does not help as far as reaching the desired *bounded* solutions, thus the need for the reaction-diffusion equations that do exhibit traveling wave solutions.

Now let us take the Fisher equation

$$\frac{\partial u}{\partial t} = ku(1 - u) + D \frac{\partial^2 u}{\partial x^2} \quad (2.51)$$

Chapter 2. A Survey of Some Current Topics in Ecology and Epidemics

which was suggested by Fisher in 1937 as a deterministic version of a stochastic model for the spatial spread of a favored gene in a population [10]. It is the logistic equation for growth population when it disperses via *linear diffusion*. After rescaling this equation to get rid of k and D , and using linear stability analysis, always considering

$$\lim_{z \rightarrow \infty} U(z) = 0, \quad \lim_{z \rightarrow -\infty} U(z) = 1, \quad (2.52)$$

we find two singular points $(0,0)$ and $(1,0)$, which are the steady states, with a minimum wave speed of $c_{min} = 2$ [10]. As suggested by Mollison (1977), to study the dependence of the wave speed c on the initial conditions at infinity, we consider the leading edge of the evolving wave where, since u is small, we can neglect u^2 in comparison with u . The dispersion relation, an expression relating a and c , is

$$c = a + \frac{1}{a}, \quad (2.53)$$

where a comes from the initial condition $u(x,0) = Ae^{-ax}$, $x \rightarrow \infty$. If we now look at a small parameter ϵ in the equations, $\epsilon = 1/c^2 \leq 0.25$, we can look for asymptotic solutions for $0 < \epsilon \ll 1$. If $z = 0$ where $U = 1/2$, and we use a standard singular perturbation technique [10,12],

$$U(z) = g(\xi), \quad \xi = z/c = \epsilon^{1/2}z. \quad (2.54)$$

The solution up to the first term is $(1 + e^{z/c})^{-1}$, which is pretty close to the computed wavefront solution of Fisher's equation [10]. There is a clear relationship between the wave speed and steepness of the wavefront at $z = 0$:

$$-U'(0) = s = \frac{1}{4c} + O\left(\frac{1}{c^5}\right), \quad c \geq 2. \quad (2.55)$$

So the *faster* the wave moves, the *less steep* the wavefront is. Now, in Chapter 3 we will find density-dependent diffusion, so a more realistic model would be an expression of the form

$$\frac{\partial u}{\partial t} = f(u) + \frac{\partial}{\partial x} \left[D(u) \frac{\partial u}{\partial x} \right], \quad D(u) = D_0 u^m, \quad f(u) = ku^p(1 - u^q). \quad (2.56)$$

Writing the full diffusion term, we get

$$\frac{\partial u}{\partial t} = u^p(1 - u^q) + mu^{m-1} \left(\frac{\partial u}{\partial x} \right)^2 + u^m \frac{\partial^2 u}{\partial x^2}, \quad (2.57)$$

which clearly shows that the nonlinear diffusion can be thought of as contributing an equivalent convection with velocity $-mu^{m-1}\partial u/\partial x$. The case where we have again our beloved logistic population growth,

$$\frac{\partial u}{\partial t} = u(1 - u) + \frac{\partial}{\partial x} \left[u \frac{\partial u}{\partial x} \right], \quad (2.58)$$

tells us that the population disperses to regions of lower density more rapidly as the population gets more crowded [10]. This remarkable phenomenon will be studied in much more detail in Chapter 3 when we analyze the results of our data for mice diffusing on the landscape in the context of the Hantavirus epidemic.

2.4.3 The SI model for epidemics

Overview

We start with the assumption that we only have susceptible (non-infected) and infected organisms within our population. $M_S(x, t)$ and $M_I(x, t)$ are the population densities of susceptible and infected organisms, respectively, and $M(x, t) = M_S(x, t) + M_I(x, t)$ is the total population.

An Example of an SI model: the AK Model

The AK model [5], named after its authors Abramson and Kenkre, is a very successful model that was developed to understand the infection of Hantavirus in deer mice, *Peromyscus maniculatus*, based on biological observations in the North American Southwest. The basic model, an SI model [10] introduced in [5] is given by the

following expressions:

$$\frac{\partial M_S(x, t)}{\partial t} = bM - cM_S - \frac{M_S M}{K(x)} - aM_S M_I + D_S \nabla^2 M_S, \quad (2.59)$$

$$\frac{\partial M_I(x, t)}{\partial t} = -cM_I - \frac{M_I M}{K(x)} + aM_S M_I + D_I \nabla^2 M_I. \quad (2.60)$$

Some key features of this model are the following:

- $M_S(x, t)$ and $M_I(x, t)$ are the population densities of susceptible and infected mice, respectively, and $M(x, t) = M_S(x, t) + M_I(x, t)$ is the total mice population.
- Births: bM represents births of mice, all of them born susceptible, at a rate proportional to the total density, since all mice contribute equally to the procreation.
- Deaths: c represents the rate of *natural* death, mice don't die from infection.
- Competition: $-M_{S,I}M/K$ represents a limitation process in the population growth, due to competition for shared resources. It is formed by a mouse of the corresponding class and one mouse of any class (since they have to compete with the whole population). K is called the *environmental parameter*: higher values represent more resources and less competition.
- Infection: $aM_I M_S$ represents the number of susceptible mice that get infected due to an encounter with an infected mouse, at some rate a .
- Diffusion: there are separate diffusion coefficients D_S and D_I for the two classes of mice.
- Infected mice do not die of infection, and infected mice are infectious for their whole lives. Infection is believed to be transmitted through aggression.

Adding Eqs.(2.59, 2.60) we get

$$\frac{\partial M(x, t)}{\partial t} = (b - c)M \left(1 - \frac{M}{(b - c)K} \right) + D\nabla^2 M, \quad (2.61)$$

the Fisher equation for the whole population, widely used to describe self-limitating populations [5, 10]. The critical value of the environmental parameter is given by

$$K_C = \frac{b}{a(b - c)}. \quad (2.62)$$

For environmental parameters above this value, so-called *refugia* appear [5]. Infection persists only in these regions and disappears for regions where the resources fall below K_C .

The Modified AK Model

As a result of the saturation of the mean square displacement in time, it was concluded that mice were moving within home ranges [3, 16, 17]. The basic idea [8, 9] is to replace the diffusion terms by corresponding terms of a Fokker-Planck equation:

$$D\nabla^2 M \Rightarrow \vec{\nabla} \cdot (D\vec{\nabla} M + M\vec{\nabla} U) = f(M), \quad (2.63)$$

where $U(x)$ is an *attractive* potential that represents the home ranges of mice.

$$\frac{\partial M_S(x, t)}{\partial t} = bM - cM_S - \frac{M_S M}{K} - aM_S M_I + f(M_S), \quad (2.64)$$

$$\frac{\partial M_I(x, t)}{\partial t} = -cM_I - \frac{M_I M}{K} + aM_S M_I + f(M_I), \quad (2.65)$$

and the sum gives us

$$\frac{\partial M(x, t)}{\partial t} = (b - c)M(x, t) - \frac{M^2(x, t)}{K} + D\nabla^2 M(x, t) + \vec{\nabla} M(x, t) \cdot \vec{\nabla} U(x) + M(x, t) \nabla^2 U(x). \quad (2.66)$$

The terms are the following:

- $(b - c)M$: growth term for the population if $b > c$.
- M^2/K : limits the growth of the population through competition of resources K .
- $D\nabla^2 M$: diffusion term that acts to homogenize the mice population.
- $\vec{\nabla}M(x, t) \cdot \vec{\nabla}U(x)$: convection term. The “velocity” $\vec{\nabla}U(x)$ acts like a wind forcing the mice to travel toward the center of their home range.
- $M(x, t)\nabla^2 U(x)$: pseudo-growth term because it multiplies the density. Effectively increases the growth rate $(b - c)$, meaning increased protection from the home range.

An attractive potential used to describe the home ranges is [8, 9]

$$U(x) = A \cos\left(\frac{2\pi x}{\lambda}\right). \quad (2.67)$$

The second derivative of a sinusoidal is maximal at the bottom of the potential, so the increased growth term is maximal at the center of the home range (max. amount of protection or defense from predators). A sinusoidal potential represents multiple home ranges, a situation that is not entirely representative of field data. More work is necessary in this context.

2.4.4 The SIR model for epidemics

Overview

Let us suppose we have a population of organisms that can be divided into *susceptibles*, those who can get the disease, *infectives*, those who have the disease and can transmit it, and *removed*, those who have had the disease or have recovered from it and are either immune or isolated from the rest of the population (they have been

Chapter 2. A Survey of Some Current Topics in Ecology and Epidemics

removed from the *risk* of being infected, NOT from the population). The progress of infection can be described by [10]

$$S \rightarrow I \rightarrow R, \tag{2.68}$$

thus the name of the model. Now let us make the following assumptions [10]:

- The gain in the number of infective individuals is proportional to infective and susceptible organisms; susceptible organisms are lost at the same rate.
- The rate of infectives that are *removed* is proportional to the number of infectives.
- The incubation period, a crucial factor in the spread of any epidemic, is negligible in this case, so a susceptible organism that contracts the disease can infect another susceptible right away.
- The probability of an organism contacting another one is the same for every pair of individuals.

Now let us proceed to modeling our epidemic. If $S(t), I(t), R(t)$ are the three classes we study in our model which depend on time,

$$S(t) + I(t) + R(t) = N, \tag{2.69}$$

where N is the total size of the population. The time evolution of the three classes can be modeled as follows [10]:

$$\frac{dS}{dt} = -rSI, \tag{2.70}$$

$$\frac{dI}{dt} = rSI - aI, \tag{2.71}$$

$$\frac{dR}{dt} = aI, \quad (2.72)$$

where $a > 0$ is the *removal rate of infectives* and $r > 0$ is the *infection rate of susceptibles*. It can be seen that

$$\frac{dS}{dt} + \frac{dI}{dt} + \frac{dR}{dt} = 0, \quad (2.73)$$

so the population N is conserved at all times [10]. The initial conditions for our model are

$$S(0) = S_0 > 0, \quad I(0) = I_0 > 0, \quad R(0) = 0, \quad (2.74)$$

so we start with susceptible and infected individuals *only*. Now comes the crucial part of the model and in fact *of any successful epidemic model*: We want to know, given certain initial conditions, whether there will be a spread of the epidemic or not, as times goes by. To fully address this issue we have

$$\left[\frac{dI}{dt} \right]_{t=0} = I_0 (rS_0 - a) \begin{cases} \geq 0 & \text{if } S_0 \geq \rho = \frac{a}{r} \\ < 0 & \text{if } S_0 < \rho \end{cases} \quad (2.75)$$

We also know that $dS/dt \leq 0, S \leq S_0$, so we have, if $S_0 < \rho$,

$$\frac{dI}{dt} = I(rS - a) \leq 0, \quad t \geq 0, \quad (2.76)$$

so the initial number of infectives, I_0 , will be greater than $I(t)$ which goes to zero as $t \rightarrow \infty$, so in this case there *cannot* be an epidemic. Now, if $S_0 > \rho$, then $I(t)$ increases with time and an epidemic will certainly occur. In fact we use the word “epidemic” whenever $I(t) > I_0$ for $t > 0$ (see Fig. 1). The parameter $\rho = a/r$, of paramount importance in this model, is called the *relative removal rate*, and its reciprocal $\sigma = r/a$ is called the *contact rate*. One important relation that can be derived from our original model is [10]

$$\frac{dI}{dS} = -\frac{(rS - a)I}{rSI} = \frac{\rho}{S} - 1, \quad I \neq 0, \quad (2.77)$$

and by integrating this equation we get

$$I + S - \rho \ln S = I_0 + S_0 - \rho \ln S_0 = \text{const.}, \quad (2.78)$$

which gives us an expression for the phase plane trajectories in (I, S) space. Another key concept in the mathematical modeling of epidemics is the *severity* of the epidemic (within the population) [10]. I_{max} , the maximum value for I , occurs when $dI/dt = 0, S = \rho$,

$$I_{max} = N - \rho + \rho \ln \left(\frac{\rho}{S_0} \right). \quad (2.79)$$

So going back we see that if $S_0 > S_c = \rho$, there is an epidemic, whereas if $S_0 < S_c = \rho$, there can't be one because the infective class is decreasing in time. Now, it will be severe (within the given population) if I_0 and I_{max} are not close to each other, and not severe if they are relatively close. Another important parameter in the study of epidemics has to do with the removal rate, which can be expressed as

$$\frac{dR}{dt} = aI = a(N - R - S) = a(N - R - s_0 \exp(-R/\rho)), \quad R(0) = 0. \quad (2.80)$$

However, given the lack of knowledge of some of the parameters involved in this equation, it has been suggested [10] that, for relatively small epidemics (R/ρ small),

$$R(t) = \frac{\rho^2}{S_0} \left[\left(\frac{S_0}{\rho} - 1 \right) + \alpha \tanh \left(\frac{\alpha at}{2} - \phi \right) \right], \quad (2.81)$$

where the parameters are given as follows:

$$\alpha = \left[\left(\frac{S_0}{\rho} - 1 \right)^2 + \frac{2S_0(N - S_0)}{\rho^2} \right]^{1/2}, \quad \phi = \frac{\tanh^{-1} \left(\frac{S_0}{\rho} - 1 \right)}{\alpha}. \quad (2.82)$$

Application of the SIR model: British School Flu Epidemic

According to [10], back in 1978 there was a flu epidemic in a British boys boarding school. The population was $N = 763$, and $I_0 = 1$, which means one boy initiated

the whole epidemic, and a total of 512 boys were confined to bed in a 2-week period! When a boy was infected, he was confined to bed immediately, thus we can have $I(t)$ directly from the data. $S_0 = 762$, $\rho = 202$, $r = 2.18 \times 10^{-3}/\text{day}$, and since $S_0 > \rho$ there is clearly an epidemic, in fact a severe one.

2.5 Spatial Models: Reaction-Diffusion and The Existence of a Minimal Domain Size

A central problem of theoretical ecology is the relation between the interactions among organisms (and their environment) and population distributions and community structures [1, 2]. Thus the role of *space* is vital in trying to solve this problem. Many mathematical models have been used to understand this, including cellular automata [1, 2], reaction-diffusion equations [1, 2, 8, 10], interacting particle systems [1], etc. Different hypotheses regarding the structure and scale of the environment and the motion of organisms about that environment characterize these models [1].

The existence of a minimal domain size is important in order to support positive species density profiles. Since space is of paramount importance here, structure and size of habitats affect the *persistence* and *extinction* of populations.

In the previous section we studied traveling waves, the first of three applications of reaction-diffusion equations in the context of spatial ecology. In this section we will study the second application: the effects of size, shape and heterogeneity of the environment on the persistence of species and community structures [1]. The idea that the size of a minimal patch can be predicted that will sustain a given population appears to be first given by [18, 19].

Before we proceed with our topic of study, we might wonder when should we use reaction-diffusion equations and when should we use other methods available in the

literature [1, 2, 10]. An often expressed view is that, if we want to achieve very detailed predictions about a certain ecological problem, we should use computer-based models such as cellular automata, interacting particle systems, or what is called individual-based or agent-based models. These models can be used to generate artificial datasets so observables, such as the mean square displacement, can be extracted later¹. In this view, reaction-diffusion models are recommended [1] for the sake of generality and insight into the mechanisms behind the predictions. The situation is, however, much more complex and neither the author nor his advisor subscribe to this view. Because it would take us far afield we will not provide any further discussions of this issue here.

Let us think in terms of a “patch”, that is some spatial region that due to spatial heterogeneity can be distinguished from its surroundings [1, 2, 10]. The patch has an edge, and the boundary conditions of the equations will be those on the edge of the patch.

2.5.1 Boundary Conditions

Fick’s law is related to the idea that the rate of diffusion across an interface is given by $\vec{J} \cdot \vec{n}$, where \vec{n} is the normal unit vector to the interface. If the density u of the population we are studying diffuses at a rate $D(x)$ and experiences *advective* behavior with velocity $\vec{v}(x)$, then the flux is given by

$$\vec{J} = -D(x)\nabla u + \vec{v}(x)u. \tag{2.83}$$

This is our constitutive relationship for the continuity equation,

$$\frac{\partial u}{\partial t} + \nabla \cdot \vec{J} = 0, \tag{2.84}$$

¹This is not the case for the present thesis (see Chapter 3), where *real* data were used to analyze the diffusion of the deer mice and then an observable, the diffusion constant, was extracted from the data.

and substituting the flux into this equation, we get

$$\frac{\partial u}{\partial t} = -\nabla \cdot \vec{J} = \nabla \cdot D(x)\nabla u - \nabla \cdot (\vec{v}(x)u), \quad (2.85)$$

the evolution equation for u , a type of diffusion equation. The boundary conditions for this equation relate the flux of individuals across a given boundary to the density at the same boundary. Using the standard notation of the reaction-diffusion literature [1], Ω will be our bounded region, $\partial\Omega$ will be its boundary, and \vec{n} will be the outward pointing normal unit vector. The flux across the boundary $\partial\Omega$ at a given point is proportional to the density at the boundary:

$$\vec{J} \cdot \vec{n} = \beta(x)u, \quad (2.86)$$

where $\beta(x)$ is a proportionality constant. If $\beta(x) = 0$, the flux across $\partial\Omega$ vanishes, which means the boundary becomes a perfect barrier avoiding any type of dispersal of the individuals. This is also called a reflecting boundary condition. If along with $\beta(x) = 0$, $\vec{v} = 0$, then $\frac{\partial u}{\partial \vec{n}} = 0$ and this is called a Neumann condition in the literature [1, 2, 10]. If $\beta(x)$ increases, more individuals cross the boundary in the direction of \vec{n} . If $\beta(x) \rightarrow \infty$, and we rewrite Eq. 2.86 as

$$u = \frac{1}{\beta(x)} \vec{J} \cdot \vec{n}, \quad (2.87)$$

we can see that the population density u vanishes on the boundary $\partial\Omega$. In other words, individuals who reach the boundary will cross it *immediately*, thus the density on the boundary remains effectively equal to zero. This is an absorbing or Dirichlet condition, also said to correspond to a *lethal* boundary in the ecological literature [1], since individuals that encounter the boundary die. If we substitute Eq. 2.83 into Eq. 2.86, we get

$$[-D(x)\nabla u + \vec{v}(x)u] \cdot \vec{n} = \beta(x)u, \quad (2.88)$$

where $\nabla u \cdot \vec{n}$ is the directional derivative of the density u in the direction of \vec{n} , and is denoted by $\frac{\partial u}{\partial \vec{n}}$. Thus, we can express the boundary condition for Eq. 2.85 as

$$D(x)\frac{\partial u}{\partial \vec{n}} + [\beta(x) - \vec{v}(x) \cdot \vec{n}(x)]u = 0. \quad (2.89)$$

If we want to rewrite the logistic model (see Eq. 2.61) using an absorbing boundary condition and a diffusion coefficient and birth and death rates that depend on space, we have [1]

$$\begin{aligned} \frac{\partial u}{\partial t} &= \nabla \cdot D(x)\nabla u + [a(x) - b(x)u]u & \text{in } \Omega \times (0, \infty) \\ u &= 0 & \text{on } \partial\Omega \times (0, \infty) \\ u(x, 0) &= u_0(x) & \text{on } \Omega. \end{aligned} \tag{2.90}$$

2.5.2 The Eigenvalue Approach

Let us start by looking at a model where $u(x, t)$ is the population density on the patch or region Ω . Let us assume a lethal exterior, that is, if individuals cross the boundary $\partial\Omega$, they die. r is the intrinsic growth rate of the population, and the individuals move on the patch with diffusion coefficient D [1, 18, 19]:

$$\begin{aligned} \frac{\partial u}{\partial t} &= D\frac{\partial^2 u}{\partial x^2} + ru & \text{in } \Omega \times (0, \infty) \\ u &= 0 & \text{on } \partial\Omega \times (0, \infty). \end{aligned} \tag{2.91}$$

This type of model is called a KISS model (acronym for the authors' initials). Since we have a boundary condition, there is spatial heterogeneity. The related eigenvalue problem is

$$\begin{aligned} \sigma\psi &= D\frac{\partial^2 \psi}{\partial x^2} + r\psi & \text{in } \Omega \\ \psi &= 0 & \text{on } \partial\Omega. \end{aligned} \tag{2.92}$$

Solutions to Eq. 2.91 can be found by using the method of separation of variables in terms of the solutions to Eq. 2.92. According to [1, 20], Eq. 2.92 admits a nonzero solution ψ *only* for certain values of σ . A solution to Eq. 2.92 includes an eigenvalue σ and a nonzero eigenfunction $\psi(x)$. Given smoothness conditions [1] and other mathematical assumptions [20], Eq. 2.92 has an infinite number of eigenvalues

$$\sigma_1 > \sigma_2 \geq \sigma_3 \geq \dots \geq \sigma_k \geq \dots \quad \text{with } \sigma_k \longrightarrow -\infty, k \rightarrow \infty. \tag{2.93}$$

Chapter 2. A Survey of Some Current Topics in Ecology and Epidemics

If ψ is a solution to Eq. 2.92, the same can be said about $c\psi$, where c is an arbitrary constant. Also, the eigenfunctions are normalized, meaning

$$\int_{\Omega} \psi^2 dx = 1. \quad (2.94)$$

According to [1,20], solutions to Eq. 2.91 can be written as

$$u(x, t) = \sum_{k=1}^{\infty} u_k e^{\sigma_k t} \psi_k(x), \quad (2.95)$$

where the numbers u_k depend on the initial condition $u(x, 0)$. The number σ_1 is called the *principal eigenvalue* and is the largest of all eigenvalues of Eq. 2.93. The associated eigenfunction ψ_1 is always positive [20] within the patch Ω . If $\sigma_1 < 0$, according to Eq. 2.93 all other eigenvalues will be negative, which means the solution given by Eq. 2.95 will decay exponentially. If, on the other hand, $\sigma_1 > 0$, the solution to Eq. 2.91 will grow exponentially. The former case is called *extinction* and the latter *persistence* of the population density within the patch Ω .

An Example in 1-D

Let us look at a one-dimensional example of this procedure [1]. Let Ω be the interval $(0, l)$ (one spatial dimension). Eq. 2.92 becomes

$$\sigma\psi = D \frac{\partial^2 \psi}{\partial x^2} + r\psi. \quad (2.96)$$

There are nonzero solutions that satisfy the boundary conditions only if, for some integer k ,

$$\sigma = \sigma_k = r - D \frac{\pi^2 k^2}{l^2}. \quad (2.97)$$

In this case the eigenfunction is given by

$$\psi_k = \frac{2}{l} \sin\left(\frac{\pi k x}{l}\right). \quad (2.98)$$

The principal eigenvalue is given by

$$\sigma_1 = r - D \frac{\pi^2}{l^2}, \quad (2.99)$$

so $\sigma_1 > 0$ only if $l > \pi \sqrt{\frac{D}{r}}$. This number is the *minimum patch size* necessary to support a population. If a patch is to be smaller than this value, the density would be close enough to the boundary $\partial\Omega$ that the loss rate of individuals from dispersal out of the patch, $D \frac{\pi^2}{l^2}$, is greater than the local growth rate r . This means σ_1 would be negative and the population would become extinct [1].

An Example in 2-D

If we consider our patch Ω to be a square of area A , the principal eigenvalue, for the associated eigenvalue problem (see Eq. 2.92) is given by [1]

$$\sigma_1 = r - dD \frac{\pi^2}{A}, \quad (2.100)$$

and the associated eigenfunction is given by

$$\psi_1 = \frac{4}{A} \sin\left(\frac{\pi x}{\sqrt{A}}\right) \sin\left(\frac{\pi y}{\sqrt{A}}\right). \quad (2.101)$$

For there to be persistence of the population within the patch, $\sigma_1 > 0$, only possible if $A > 2D \frac{\pi^2}{r}$. This is the minimum patch size for the two-dimensional case of a square patch of area A .

The Scaling Problem

If we look at Eqs. 2.99 and 2.100, it is evident that the two principal eigenvalues we just derived depend on the geometry of the patch (l, A) and the biological parameters of the population (r, D). In order to separate the two effects [1] proposes the

associated eigenvalue problem

$$\begin{aligned} \frac{\partial^2 \phi}{\partial x^2} + \lambda \phi &= 0 & \text{in } \Omega \\ \phi &= 0 & \text{on } \partial\Omega. \end{aligned} \tag{2.102}$$

If we assume that ϕ is an eigenfunction of Eq. 2.102, and we set $\psi = \phi$, we get

$$D \frac{\partial^2 \phi}{\partial x^2} + r\psi = (r - D\lambda) \psi. \tag{2.103}$$

This means the eigenvalues of Eq. 2.92 and those of Eq. 2.102 are related by the expression

$$\sigma = r - D\lambda, \tag{2.104}$$

and the fact that $\sigma_1 > 0$ is now $\frac{r}{D} > \lambda_1$, where λ_1 is the principal eigenvalue for Eq. 2.102. According to Strauss (1992) and [1], Eq. 2.102 has eigenvalues

$$\lambda_1 < \lambda_2 \leq \lambda_3 \leq \dots, \tag{2.105}$$

and λ_1 is the only eigenvalue with a positive eigenfunction. In the 1-dimensional case, $\lambda_1 = \frac{\pi^2}{l^2}$. In the 2-dimensional case, $\lambda_1 = 2\frac{\pi^2}{A}$. If we look carefully at these two eigenvalues we notice they go as $\frac{1}{l^2}$. It can be proven [1] that if we take a *rescaled* version of Eq. 2.102, i.e.,

$$\begin{aligned} \frac{\partial^2 \tilde{\phi}}{\partial x^2} + (\lambda/l^2) \tilde{\phi} &= 0 & \text{in } \tilde{\Omega} \\ \tilde{\phi} &= 0 & \text{on } \partial\tilde{\Omega}, \end{aligned} \tag{2.106}$$

the eigenvalues for this system are given by

$$\tilde{\lambda}_k = \frac{\lambda_k}{l^2}, \tag{2.107}$$

where λ_k is an eigenvalue of Eq. 2.102. Thus, for a population to be able to *persist* according to the model given by Eq. 2.91 given patch $\tilde{\Omega}$ and boundary $\partial\tilde{\Omega}$ (see Eq. 2.106), the following condition is necessary:

$$\frac{r}{D} > \tilde{\lambda}_1 = \frac{\lambda_1}{l^2}, \tag{2.108}$$

which turns out to be independent of the geometry of the patch [1].

2.5.3 The Energy Method Revisited

Refs. [1, 21–23] applied the so-called *energy method* from classical mechanics to study reaction-diffusion models in one dimension in order to study the behavior of the fixed points with respect to the size of the patch Ω . Let us consider the following reaction-diffusion model with diffusion constant $D = 1$:

$$\begin{aligned} \frac{\partial u}{\partial t} &= \frac{\partial^2 u}{\partial x^2} + f(u) \quad \text{on} \quad (-l/2, l/2) \times (0, \infty) \\ u(x, t) &= 0 \quad \text{for} \quad x = \pm l/2. \end{aligned} \tag{2.109}$$

If we take the steady-state solution and multiply on both sides by du/dx , we obtain

$$\begin{aligned} 0 &= \frac{d^2 u}{dx^2} \frac{du}{dx} + f(u) \frac{du}{dx} \\ &= \frac{d}{dx} \left[\frac{1}{2} \left(\frac{du}{dx} \right)^2 + F(u) \right], \end{aligned} \tag{2.110}$$

where

$$F(u) = \int_0^u f(s) ds. \tag{2.111}$$

From Eq. 2.110 we conclude that

$$\frac{1}{2} \left(\frac{du}{dx} \right)^2 + F(u) = \text{const.} \tag{2.112}$$

In physics this constant is called the *energy* of the system. If u is a fixed point of the system given by Eq. 2.109, then $u(x, t)$ must reach a maximum within the patch Ω [1], denoted from now on by u_{max} . We must have

$$\frac{1}{2} \left(\frac{du}{dx} \right)^2 + F(u) = F(u_{max}) \tag{2.113}$$

since $\frac{du}{dx} = 0$ at u_{max} . Also, $F(u_{max}) \geq F(u)$ for $0 \leq u \leq u_{max}$ since $u(x)$ takes all values from 0 to u_{max} . If $f(u) > 0$ for $0 < u < K$ but $f(u) < 0$ for $u > K$, then $F(u) < F(u_{max})$, except for $u = u_{max}$ [1]. If $u(x_0) = u_{max}$, then, solving for du/dx in Eq. 2.113, we get

$$\begin{cases} \sqrt{2} \sqrt{F(u_{max}) - F(u)} & \text{for} \quad -l/2 < x < x_0 \\ -\sqrt{2} \sqrt{F(u_{max}) - F(u)} & \text{for} \quad x_0 < x < l/2. \end{cases} \tag{2.114}$$

According to [1], if we take $x_0 = 0$, we get

$$l = \sqrt{2} \int_0^{u_{max}} \frac{du}{\sqrt{F(u_{max}) - F(u)}}, \quad (2.115)$$

so for different nonlinearities $f(u)$, this expression is useful to analyze the relationship between u_{max} and the length l of the patch.

Logistic Growth Revisited

Let us look again at the phenomenon of logistic growth in a population, and let us analyze it in the light of the results yielded by the application of the energy method. Our nonlinearity is

$$f(u) = r \left(1 - \frac{u}{K}\right) u = ru - \frac{r}{K} u^2. \quad (2.116)$$

$$F(u) = r \frac{u^2}{2} - \frac{r}{3K} u^3. \quad (2.117)$$

If we make the substitution $w = u/u_{max}$ [1], Eq. 2.115 becomes

$$l = \sqrt{2} \int_0^1 \frac{u_{max} dw}{\sqrt{F(u_{max}) - F(wu_{max})}} = \sqrt{2} \int_0^1 \frac{dw}{\sqrt{\frac{F(u_{max}) - F(wu_{max})}{u_{max}^2}}}, \quad (2.118)$$

and using Eq. 2.117 and substituting terms we get

$$l = \sqrt{2} \int_0^1 \frac{dw}{\sqrt{\frac{r}{2}(1-w^2) - \frac{ru_{max}}{3K}(1-w^3)}}. \quad (2.119)$$

From this expression it is clear that as $u_{max} \rightarrow 0$, the integrand goes to

$$\frac{\sqrt{\frac{2}{r}}}{\sqrt{1-w^2}}, \quad (2.120)$$

thus the length of the patch, l , approaches the value $\frac{\pi}{\sqrt{r}}$. This is the *minimum patch size* for the logistic case, and it can be plotted as a function of u_{max} (see Fig. 2.9).

If $u_{max} = K$, then the patch is infinitely large, it cannot be bounded.

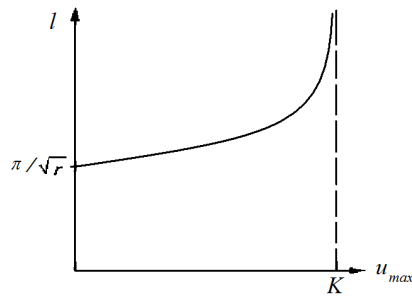


Figure 2.9: The length of the patch, l , versus the maximum density, u_{max} , for the logistic case. After Cantrell and Cosner [1].

2.6 Spatial Models: Reaction-Diffusion and Patterns

In this section we will study the third application [1, 2] of reaction-diffusion equations in the context of spatial ecology: the formation of patterns. These patterns may or may not change in time, depending on the particular assumptions made when constructing the reaction-diffusion equations [2, 10].

The concept of *invasion fitness* [2] refers to the initial per/capita growth rate of a rare mutant in a certain environment previously set by its residents. This concept, at the heart of adaptive dynamics theory, can be readily measured in populations without spatial structure. However, in populations that are spatially heterogeneous (spatially-structured), invasion fitness is heavily influenced by the patterns that arise from *short-range* ecological interactions. Our group has been very successful at predicting patterns [5–7] in several biological and physical contexts. For instance, spatial patterns or “refugia” [5] were predicted using the AK model.

As pointed out in the previous section, different models can be used to describe different ecological phenomena [1, 2, 10]. For the case of pattern formation also,

within the framework of reaction-diffusion models, we can use either partial differential equations (PDEs) or cellular automata (CA) [2]. The former are thought to be more suitable to describe processes such as the Belousov-Zhabotinsky reaction [2, 10], notorious for its intricate and often regular patterns. Also, CA models focus on *local* correlations while PDEs are large-scale descriptions of populations and therefore local correlations are often neglected [2, 10]. We will focus mainly on PDE-based models for pattern formation in the remainder of this section.

Patterns and the Origin of Life

Pattern formation occupies a major role in some models that pretend to find insight into the origin of life [2]. A biological system, for instance made up of molecules, is studied in which the spatial factor eventually drives the system to become subdivided into compartments, such that spread of infection is no longer possible due to the presence of compartments and “firewalls” between them. The general PDE model in one dimension used to describe the problem of the origin of life is given by [2]

$$\frac{\partial X_i}{\partial t} = M \sum_{j=1}^N k_{ij} X_j X_i - g_X X_i + D_X \frac{\partial^2 X_i}{\partial x^2}, \quad i = 1, \dots, N \quad (2.121)$$

$$\frac{\partial M}{\partial t} = k_M - g_M M - LM \sum_{i,j=1}^N k_{ij} X_j X_i + D_M \frac{\partial^2 M}{\partial x^2}, \quad (2.122)$$

The terms of Eq. 2.121 are explained as follows:

- X_i is the density of polymers of type i .
- M is the density of monomers.
- N is the number of species of polymers present in the system.

Chapter 2. A Survey of Some Current Topics in Ecology and Epidemics

- $M \sum_{j=1}^N k_{ij} X_j X_i$ is the catalyzed replication of polymer X_i , where the growth rate is proportional to the density of activated monomers M and to the replication of templates X_i by polymers X_j via rate constants k_{ij} .
- $-g_X X_i$ corresponds to decay of polymers, where g_X is the decay rate constant.
- $D_X \frac{\partial^2 X_i}{\partial x^2}$ is the diffusion term in one dimension, and D_X is the diffusion constant for the polymers.

The terms of Eq. 2.122, which describes the dynamics of the density of activated monomers M that limits the growth of polymers X_i are explained as follows:

- M is the density of monomers.
- k_M is the constant rate of production of monomers.
- $-g_M M$ corresponds to decay of monomers to an inactive form, where g_M is the decay rate constant.
- $-LM \sum_{i,j=1}^N k_{ij} X_j X_i$ corresponds to the consumption of monomers due to the replication of polymers; L is the number of monomers required to produce a polymer.
- $D_M \frac{\partial^2 M}{\partial x^2}$ is the diffusion term in one dimension, and D_M is the diffusion constant for the monomers, usually greater than D_X .

Results in 2 Dimensions: Spirals

Before we look at the results of the simulations performed by [2] for the system mentioned above, let us look at the very important concept of *hypercycle*. It was introduced in the early 1970s [24] and consists of a set of self-replicating molecule species X_i . The important point of this concept is the fact that each species provides

catalytic support for the next species in the hypercycle [2, 24]. Each species replicates itself and “helps” with the replication process of the next species. This was dubbed an “altruistic” process [2, 25] because it does not increase the number of copies of one given species but increases those of the competing species which the first species helps replicate. Parasites are an important part of hypercycle theory [2, 25] since they can replicate on its own like the molecular species that form the hypercycle. However, the difference lies in the fact that they receive support from some species but they won’t give it back to any other species [2] (see Fig. 2.10). Thus, if a parasite is *selected* in favor of another species, the hypercycle is gone, and this is called *evolutionary instability* [2, 25].

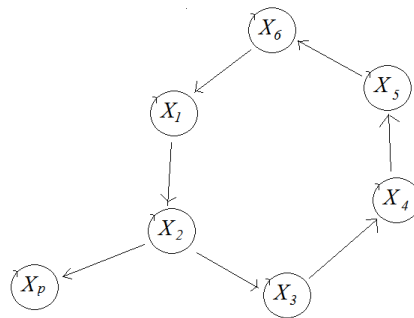


Figure 2.10: Sketch of a hypercycle with 6 self-replicating molecular species and one parasite species that gets help replicating from species 2 but won’t help anyone but itself to replicate. Based on figures from Dieckmann, Law, and Metz [2].

Now let us focus on the results of the numerical simulations of Eqs. 2.121 and 2.122 performed by [2]. It was proven by [26] that in PDE-based reaction-diffusion models such as the one mentioned above, hypercycles with 5 or more species yield spiral patterns for most initial conditions (see Fig. 2.11). When a parasite is present in the system, the spiral collapses [2].

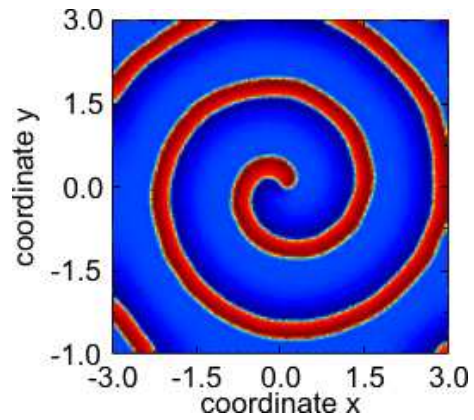


Figure 2.11: Reaction-diffusion spiral for five species. The color at each point represents the species with the highest concentration at that given point. Copyright Wikimedia Commons.

Chapter 3

Diffusion Constants of Rodents in New Mexico and Wyoming

3.1 Overview

This chapter is a report of new theoretical research carried out by the author as part of his Master's thesis. The present analysis continues the efforts of our research group to understand the behavior of the Sin Nombre Virus (Bunyaviridae: Hantavirus), which was discovered in 1993 as the agent of the deadly Hantavirus Pulmonary Syndrome (HPS) in the North American Southwest region [27]. The movement characteristics of the principal host of the virus, the deer mouse, *Peromyscus maniculatus* [28], have been studied extensively in the past. An analytical model [5, 29–31] was successfully developed and led to an understanding of spatio-temporal patterns that have been confirmed by observations in the field.

The basic assumption of that model is that the movement of the animals has a diffusive behavior, given by the diffusion constant D . This statement is supported by many previous studies of animal movement [10, 32], including studies of the deer mice

[33, 34]. A comprehensive theory [35] that formed the basis for the extraction of rodent parameters was applied in the first paper [16] of the present series (from now on referred to as I), for the analysis of field data for marked-recaptures of *Zygodontomys brevicauda* in Panama from trapping measurements in a grid arrangement.

A second application of the theory allowed an extraction of rodent parameters in a subsequent paper [3] (from now on called II), for the deer mouse *Peromyscus maniculatus* in the region of Sevilleta, New Mexico (USA). The measurement method was trapping in a *web arrangement*, a method that was thoroughly explained by Dr. Parmenter et al. [4] as a means to estimate small-mammal densities in the field (compared to the grid-based arrangement). The diffusion constant found in I was $D = 200 \text{ m}^2/\text{day}$ and the value reported in II was $D = 470 \pm 50 \text{ m}^2/\text{day}$. An additional and crucial parameter of the rodent motion that the theory allowed to extract was L , the home range size for the mice. In I it was found that $L = 70 \text{ m}$. In II, the long-time measurements show the home range size to be $L = 100 \pm 25 \text{ m}$, using the box model introduced in I for home range estimation. We were not able to find home range parameters when analyzing the datasets reported in the present Chapter, given the absence of a saturation value for the mean square displacement as a function of time.

3.2 Recapture of animals and displacement measurement

Our interest in the present Chapter is in the extraction of rodent quantities from field data gathered between June 2004 and May 2007 at the Valles Caldera National Preserve in New Mexico (New Mexico from now on), and between June 1982 and August 1985 in the Wyoming grassland (Wyoming from now on). For New Mexico,

Chapter 3. Diffusion Constants of Rodents in New Mexico and Wyoming

nine trapping webs were permanently set on the terrain (see Fig. 3.1) and animals were captured on a monthly basis for three consecutive nights on each occasion. Eight species of rodents were recaptured for the present analysis:

- *Peromyscus maniculatus* (deer mouse)
- *Tamias minimus* (chipmunk)
- *Tamias quadrivittatus*
- *Reithrodontomys megalotis*
- *Neotoma mexicanus*
- *Neotoma cinereus*
- *Microtus longicaudus*
- *Spermophilus lateralis*

However, only *P. maniculatus* yielded enough data to calculate the diffusion constant of their movement. The data set contained 261 recaptures of *P. maniculatus* (114 in the first, 86 in the second, and 61 in the third year), compared to 3765 in II. There were 112 female and 149 male recaptures. The recaptures of deer mice included 191 adult and 70 juveniles, the cut-off between the two being a body mass of 16 grams. This is important because we performed analyses over the two age-groups and we also found diffusion constants for each of several years.

For Wyoming, there were three replicate square grids, labeled as North, Middle, and South. The sites were sampled twice per year, once in Spring (May-July dates) and once in late summer (August-September dates). Traps were run for four nights, with traps being opened on a Monday, and checked each morning from Tuesday through Friday. The deer mouse was the only rodent species present in the area, so

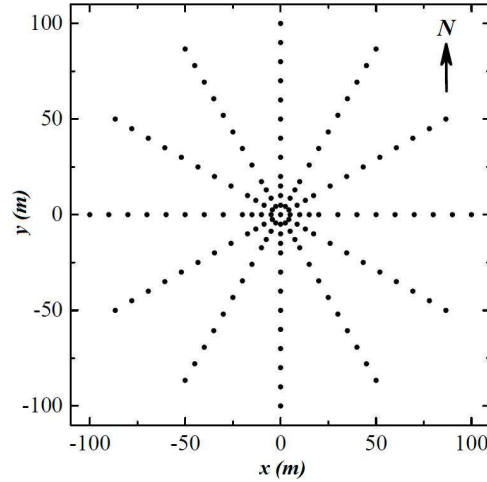


Figure 3.1: Schematic arrangement of each of the 9 trapping webs used to obtain the New Mexico dataset. Each dot represents a Sherman trap. There is only one trap at the center as opposed to four traps in II. The four inner circles have radii increasing in 5 m intervals, while the rest are separated by 10 m. There are 145 traps per web. [3, 4].

only this species contributed to the Wyoming dataset. It contained 272 recaptures in 1982, 537 in 1983, 192 in 1984, and 191 in 1985, for a total of 1192 recaptures. There were 666 female and 526 male recaptures, and 250 juvenile and 942 adult recaptures. As in New Mexico, the cut-off between the two age-groups was a body mass of 16 grams.

The mark-recapture data analyzed here come from the use of trapping webs such as the one shown in Fig. 3.1 for New Mexico and grids for Wyoming, as seen in Fig. 3.2. This involves the implementation of the “distance sampling” method [36], also used in II. The web configuration has the advantage that it can be used (and is widely used) to estimate the absolute densities of rodents [4, 37]. However, for the study of animal motion this configuration presents a problem: the distribution of the traps is very inhomogeneous, as can be clearly seen in Fig. 3.1. As was first done in II, Fig. 3.3 shows the observed distribution of the displacements of deer mice at several time scales, ranging from 1 day to 3 months, compared to the distribution of distances

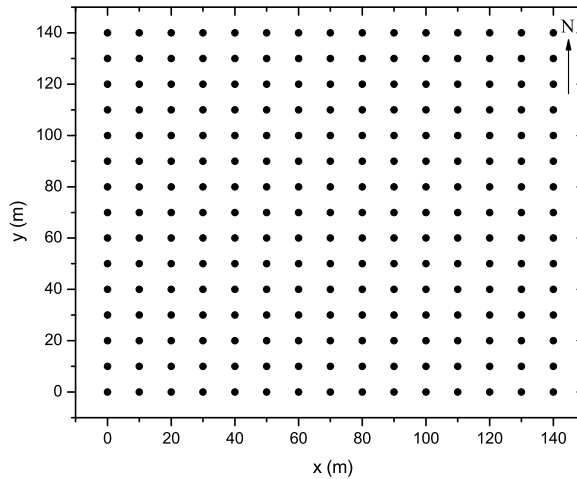


Figure 3.2: Schematic arrangement of each of the 3 square trapping grids used to obtain the Wyoming dataset. Each dot represents a Sherman trap. Each grid has 225 traps, with 10 meters between traps in the two spatial directions. Each grid has a side of length 140 m, with 100 m between each grid.

in the web (for New Mexico). There is a strong bias in the distribution of distances present in the array, as can be observed in the figure (heavy line, denoted $w(r)$). The traps were measured every month during three consecutive days, so we have several “time scales”, 1 day, 2 days, and multiples of 30 days. For the case of Wyoming, the distribution of the traps was completely homogeneous (square grid, see Fig. 3.2) and only the 1-day time-scale was present for this dataset given the frequency of the recaptures. Fig. 3.3 shows the normalized histograms of the observations for New Mexico.

As first pointed out in II, if the motion of the mice were purely diffusive, and if the measurements of the displacements were fine enough, these distributions should be decreasing Gaussians, always with a maximum at zero. The artifact produced by the web is equivalent to a repulsion at short distances, as if the animals would prefer to stay away from their initial position. This is obviously fictitious. However, it can

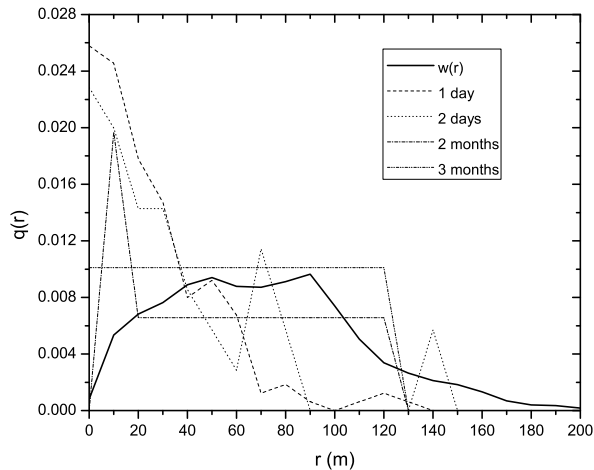


Figure 3.3: Observed distribution $q(r)$ of displacements r at several time scales, compared with the distribution $w(r)$ of distances in the web, for New Mexico.

be seen in Fig. 3.3 that for the 1-day time scale of New Mexico, the distribution of displacements has a maximum at, or very near, zero. This is a clear indication that the measurements on this time scale can be reliably used for the estimation of the diffusion coefficient, thus from now on we will refer to the 1-day scale as our “short-time-scale”.

Fig. 3.4 shows the number of distances present in the web used in New Mexico in the East-West direction (see [3] for a thorough discussion). Since the web configuration is symmetrical, the distribution in the East-West direction is identical to that in the North-South direction. Fig. 3.5 shows the number of distances present in the grid used in Wyoming in the East-West direction. Symmetry applies in this case as well.

Chapter 3. Diffusion Constants of Rodents in New Mexico and Wyoming

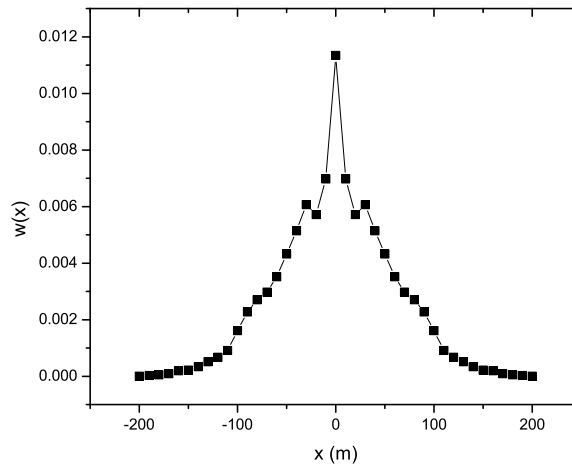


Figure 3.4: Distribution of East-West and North-South distances in the web trapping configuration (New Mexico). The diameter of the grid is 200 m.

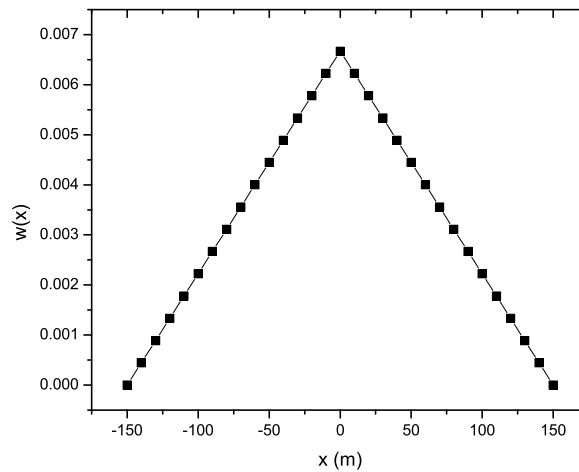


Figure 3.5: Distribution of East-West and North-South distances in the square grid trapping configuration (Wyoming). The side of the grid is 140 m.

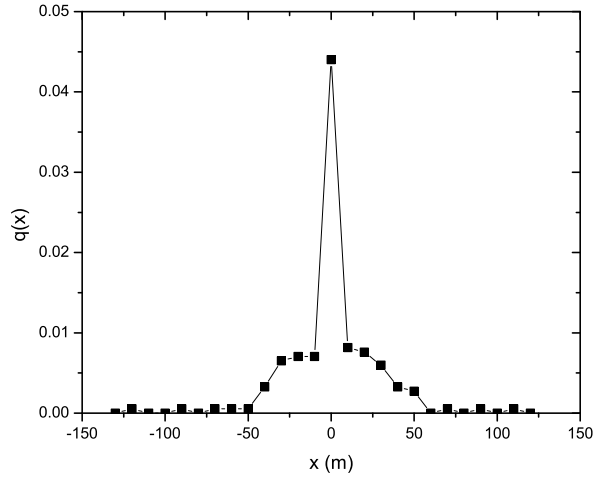


Figure 3.6: Probability distribution of observed displacements for *P. maniculatus* in the East-West direction for the 1 day time-scale (New Mexico).

3.3 Renormalization of the measurements and estimation of the diffusion constants

Following the approach used in I and II, we consider the displacements of the recaptured rodents as a statistical ensemble, representing the movement of a hypothetical mouse (a random walker) whose statistical properties we want to derive from the data. When observed on a short-time scale, the motion of the walker might be approximately diffusive for the reasons explained above. At longer times, both the existence of home ranges and the finiteness of the array take over, constraining the walk. Unfortunately, the datasets described in the present Chapter were not large enough to yield data to compute the home ranges, so only diffusion constants will be discussed here.

If we take the movement of the mice to be diffusive at short-time scales [3, 16], the probability density function of the displacements of an ensemble of mice from an

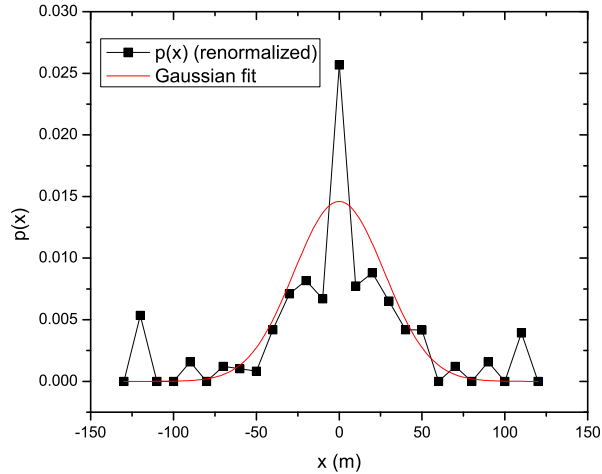


Figure 3.7: Renormalized probability distribution of actual displacements that characterizes the movement of *P. maniculatus* in the East-West direction at 1 day (New Mexico). The continuous line shows the least-squares Gaussian fit of the distribution ($\chi^2 = 1.0 \times 10^{-5}$).

initial position is just the standard (Gaussian) propagator of diffusive motion, with diffusion coefficients that are generally different in the different spatial directions due to movement anisotropy, varying conditions of the terrain, slopes, etc. One of the key points of the present analysis has to do with the fact that the measurements of position are taken with a grid of traps, which is a discrete device. As was first explained by [3], it is possible to take into account the distribution of distances between traps in the web to take the effect of the bias, as follows: the *observed* probability $Q(x) = q(x)dx$ of making a displacement between x and $x + dx$, is equal to the probability $P(x) = p(x)dx$ that, in a day's time, the random walker *actually makes* such a movement, multiplied by the probability that the web *contains* such a distance, $W(x) = w(x)dx$. Using this relation, the observations can be renormalized to obtain the distribution of displacements that characterizes the movement,

$$P(x) = \frac{Q(x)}{W(x)} = \frac{q(x)}{w(x)}. \quad (3.1)$$

Using the same procedure followed in II, the distributions $q(x)$ and $w(x)$ are built from the recapture data and from the geometry of the web, respectively (see Figs. 3.5 and 3.6 for the New Mexico dataset). Since we assumed diffusive motion, the distribution $p(x)$ is bell-shaped (see Fig. 3.7), and is well fitted by a Gaussian ($\chi^2 = 1.0 \times 10^{-5}$), supporting the hypothesis that the movement is initially diffusive. Following this hypothesis, this Gaussian distribution is nothing but the propagator of the diffusive movement process at 1 day, the shortest time scale available from both datasets.

3.4 Movement Parameters

To obtain the following movement parameters, we went through the datasets and used only *recapture* data, that is, data for rodents that were recaptured at least one time. The analysis yielded the following results:

3.4.1 Results: Wyoming

Species: <i>Peromyscus maniculatus</i>	D_x (m^2/day)	D_y (m^2/day)
Full Wyoming dataset	80 ± 10	130 ± 10
Sample 1 (1982-1)	240 ± 30	170 ± 20
Sample 2 (1982-2)	90 ± 10	270 ± 30
Sample 3 (1983-1)	70 ± 10	110 ± 10
Sample 4 (1983-2)	60 ± 10	110 ± 10
Sample 5 (1984-1)	110 ± 10	95 ± 10
Sample 6 (1984-2)	100 ± 10	110 ± 10
Sample 7 (1985-1)	160 ± 15	280 ± 30
Sample 8 (1985-2)	30 ± 5	80 ± 10

Chapter 3. Diffusion Constants of Rodents in New Mexico and Wyoming

Males Sample 1 (1982-1)	300 ± 30	280 ± 20
Males Sample 2 (1982-2)	90 ± 10	450 ± 50
Males Sample 3 (1983-1)	190 ± 20	250 ± 30
Males Sample 4 (1983-2)	60 ± 10	210 ± 20
Males Sample 5 (1984-1)	320 ± 30	120 ± 10
Males Sample 6 (1984-2)	240 ± 20	80 ± 10
Males Sample 7 (1985-1)	310 ± 30	760 ± 80
Males Sample 8 (1985-2)	120 ± 10	110 ± 10
Females Sample 1 (1982-1)	200 ± 20	70 ± 10
Females Sample 2 (1982-2)	90 ± 10	140 ± 20
Females Sample 3 (1983-1)	30 ± 20	50 ± 30
Females Sample 4 (1983-2)	50 ± 5	70 ± 10
Females Sample 5 (1984-1)	40 ± 5	80 ± 10
Females Sample 6 (1984-2)	60 ± 5	120 ± 10
Females Sample 7 (1985-1)	30 ± 5	40 ± 5
Females Sample 8 (1985-2)	20 ± 5	70 ± 10
Juveniles Sample 1 (1982-1)	220 ± 20	240 ± 20
Juveniles Sample 2 (1982-2)	—	—
Juveniles Sample 3 (1983-1)	70 ± 10	80 ± 10
Juveniles Sample 4 (1983-2)	90 ± 10	150 ± 20
Juveniles Sample 5 (1984-1)	20 ± 2	50 ± 5
Juveniles Sample 6 (1984-2)	140 ± 15	65 ± 10
Juveniles Sample 7 (1985-1)	250 ± 30	$830? \pm 80$
Juveniles Sample 8 (1985-2)	30 ± 5	90 ± 10
Adults Sample 1 (1982-1)	250 ± 30	150 ± 20
Adults Sample 2 (1982-2)	90 ± 10	260 ± 30
Adults Sample 3 (1983-1)	70 ± 10	120 ± 10

Chapter 3. Diffusion Constants of Rodents in New Mexico and Wyoming

Adults Sample 4 (1983-2)	50 ± 5	100 ± 10
Adults Sample 5 (1984-1)	120 ± 10	100 ± 10
Adults Sample 6 (1984-2)	90 ± 10	160 ± 20
Adults Sample 7 (1985-1)	150 ± 20	210 ± 20
Adults Sample 8 (1985-2)	30 ± 5	70 ± 10
Adult Males Sample 1 (1982-1)	350 ± 50	270 ± 30
Adult Males Sample 2 (1982-2)	90 ± 10	580 ± 110
Adult Males Sample 3 (1983-1)	200 ± 20	270 ± 30
Adult Males Sample 4 (1983-2)	50 ± 5	260 ± 20
Adult Males Sample 5 (1984-1)	320 ± 40	120 ± 10
Adult Males Sample 6 (1984-2)	190 ± 50	440 ± 30
Adult Males Sample 7 (1985-1)	380 ± 60	660 ± 90
Adult Males Sample 8 (1985-2)	180 ± 60	210 ± 30
Adult Females Sample 1 (1982-1)	210 ± 30	70 ± 10
Adult Females Sample 2 (1982-2)	90 ± 10	160 ± 10
Adult Females Sample 3 (1983-1)	40 ± 5	60 ± 5
Adult Females Sample 4 (1983-2)	50 ± 5	60 ± 5
Adult Females Sample 5 (1984-1)	40 ± 5	80 ± 10
Adult Females Sample 6 (1984-2)	60 ± 10	110 ± 20
Adult Females Sample 7 (1985-1)	30 ± 5	30 ± 5
Adult Females Sample 8 (1985-2)	16 ± 1	50 ± 5

Table 3.1: Diffusion constants in the two spatial directions at the short time scale (1 day) for Wyoming.

Adults vs. Juveniles (Wyoming)

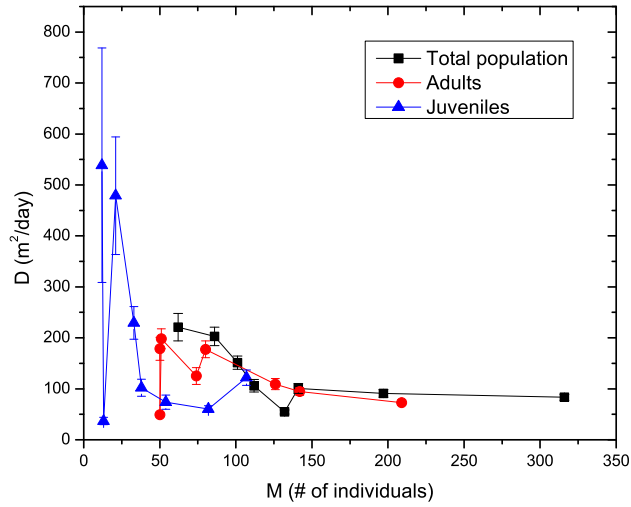


Figure 3.8: Diffusion constant vs. number of individuals for the total, adult, and juvenile populations (Wyoming).

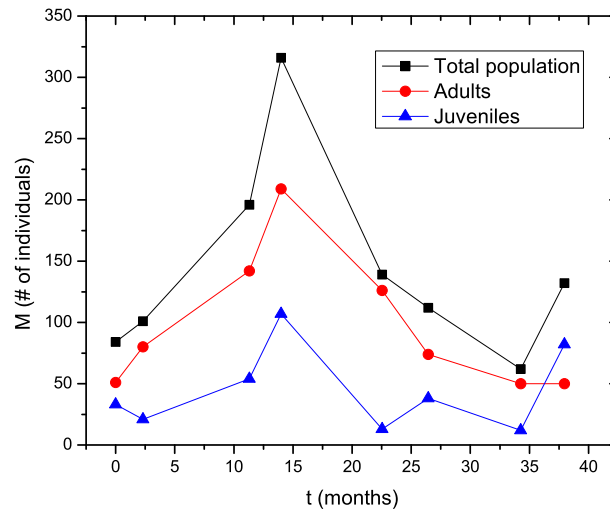


Figure 3.9: Number of individuals vs. time for the total, adult, and juvenile populations (Wyoming).

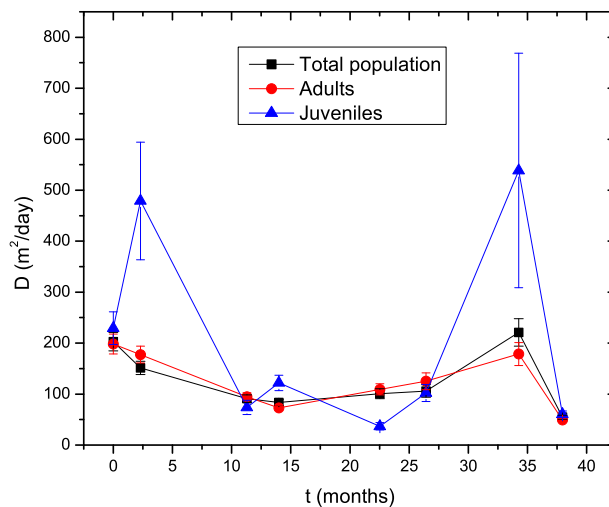


Figure 3.10: Diffusion constant vs. time for the total, adult, and juvenile populations (Wyoming).

Males vs. Females (Wyoming)

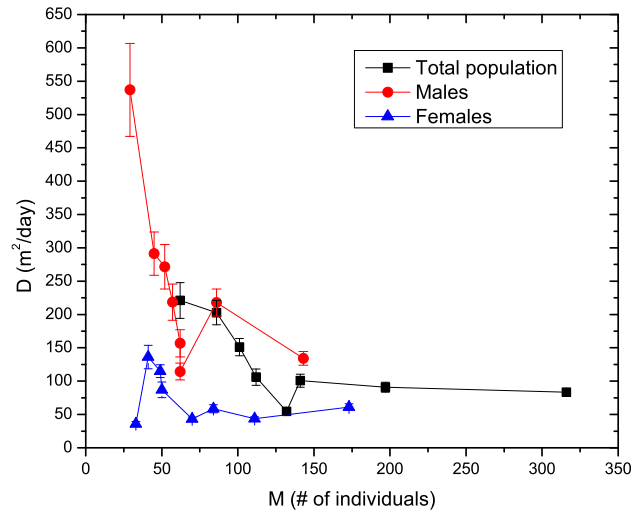


Figure 3.11: Diffusion constant vs. the number of individuals for the total, male, and female populations (Wyoming).

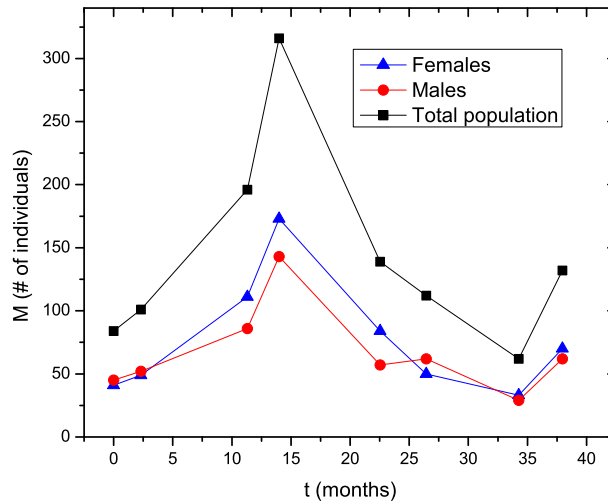


Figure 3.12: Number of individuals vs. time for the total, male, and female populations (Wyoming).

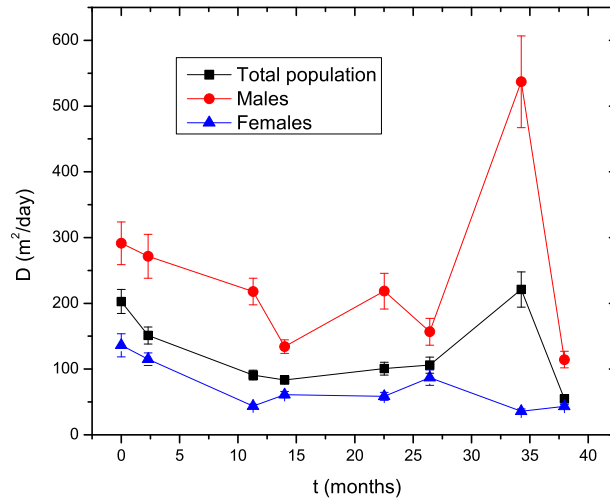


Figure 3.13: Diffusion constant vs. time for the total, male, and female populations (Wyoming).

Adult Males vs. Adult Females (Wyoming)

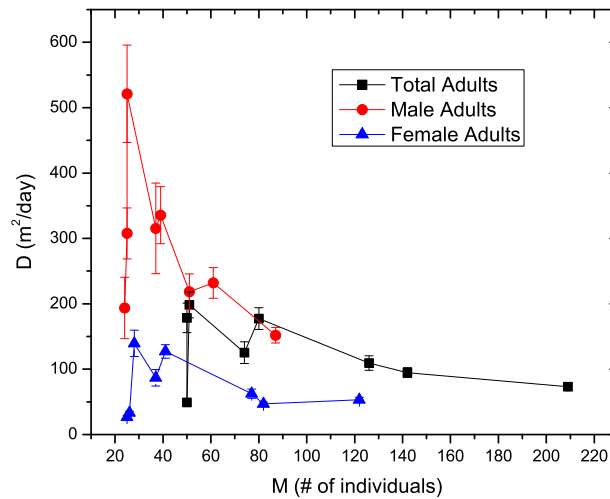


Figure 3.14: Diffusion constant vs. the number of individuals for adult males, adult females, and total adult populations (Wyoming).

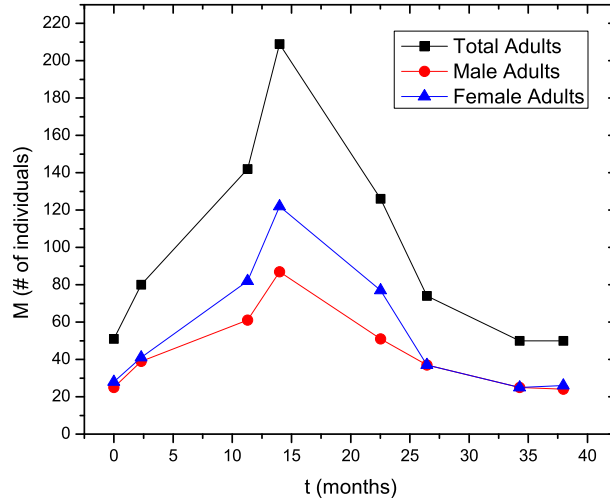


Figure 3.15: Number of individuals vs. time for adult males, adult females, and total adult populations (Wyoming).

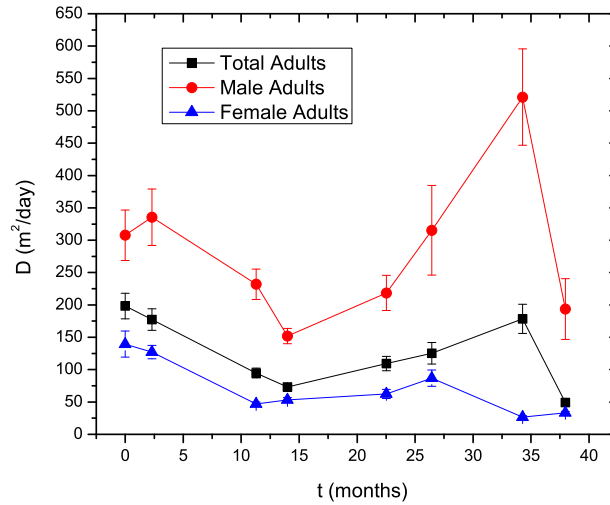


Figure 3.16: Diffusion constant vs. time for adult males, adult females, and total adult populations (Wyoming).

3.4.2 Results: New Mexico

Species: <i>Peromyscus maniculatus</i>	D_x (m^2/day)	D_y (m^2/day)
Full New Mexico dataset	340 ± 40	300 ± 40
2004-05	230 ± 30	270 ± 30
2005-06	370 ± 40	100 ± 10
2006-07	370 ± 40	370 ± 40
Males 2004-05	370 ± 40	430 ± 40
Males 2005-06	150 ± 15	90 ± 10
Males 2006-07	360 ± 40	260 ± 30
Females 2004-05	390 ± 40	150 ± 15
Females 2005-06	370 ± 40	430 ± 40
Females 2006-07	370 ± 40	430 ± 40
Juveniles	300 ± 30	280 ± 30
Adults	370 ± 40	430 ± 40

Table 3.2: Diffusion constants in the two spatial directions at the short time scale (1 day) for New Mexico.

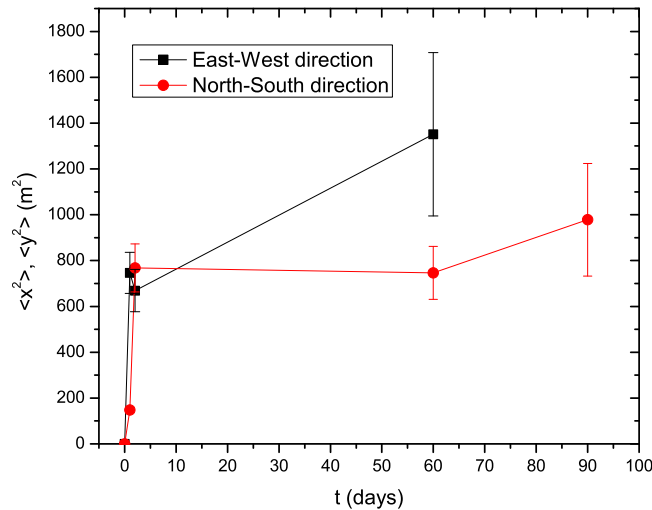


Figure 3.17: Mean square displacement in the two spatial directions as a function of time for *P. maniculatus* (New Mexico). The initial slope of each curve is $2D$, where D is the diffusion coefficient.

Chapter 4

Conclusions

These concluding remarks refer, for the most part, to the research carried out in Chapter 3 of this thesis.

From the point of view of the available resources at the different recapture sites, we can safely say Panama ($D = 200 \text{ m}^2/\text{day}$) had the most resources (I), followed by Valles Caldera National Preserve in New Mexico ($D = 320 \pm 40 \text{ m}^2/\text{day}$) (Chapter 3), and finally Sevilleta, New Mexico ($D = 470 \pm 50 \text{ m}^2/\text{day}$). We can immediately see that the less resources the mice had, the faster they moved, meaning, on average, they had to cover a greater area every day in order to look for food.

From Fig. 3.8 we can see very clearly that the diffusion constants become smaller as the population becomes larger. This observation is due to Parmenter¹. This is probably due to: (1) Food is plentiful (hence the high reproduction and subsequent densities of mice) and they don't have to venture very far from their burrows to get what they need (this has the advantage of reducing predation risk as well), and/or (2) There are so many other mice around with which to get into fights (mice usually don't like each other and fight a lot) that the increased number of encounters (and

¹Personal communication.

Chapter 4. Conclusions

fights) at high density tends to restrict their movements to the areas right near their burrows. It may also be that both of these hypotheses are operating at the same time.

Another important point has to do with the dependence of the motion of mice on their age. It is apparent that for small populations, the juveniles move much faster than for large populations, relative to the adults. It can also be concluded that, for the same number of juvenile and adult mice, adults seem to move faster. From Fig. 3.9 it is clear that for all times except that represented in the last sample, more adults than juveniles were present within the population. This supports the statement that the diffusion behavior with respect to the density mentioned above was mainly governed by the adults, not the juveniles. Fig. 3.10 shows that, throughout the four years of the study, the diffusion of the whole population was governed by that of the adult mice, and the movement of the juveniles fluctuated around the behavior of the adults and thus of the whole population.

If we look at the gender of the mice, we can see from Figs. 3.11 and 3.13 that diffusion constants in general, as we mentioned above, tend to decrease with the population. We also see that males tend to move much faster than females, probably due to the fact that females prefer to stay closer to their home. Fig. 3.12 tells us that, on average, population densities were similar, with a small domination of females over males as far as sheer number of individuals. Fig. 3.13 also shows that as time goes by, the diffusion for males and females tend to decrease and increase in a similar fashion, so on average, when they decrease for one group they do for the other, and vice versa.

For New Mexico, there was no important anisotropy in the movement regarding the two spatial dimensions, since, according to Table 1, out of the 12 values reported for New Mexico, 6 showed a dominance of the x direction and 6 a dominance of the y direction.

Chapter 4. Conclusions

It was not possible to determine home ranges from the analyzed datasets, since, according to I and II, a saturation of the mean square displacement vs. time is needed in order to predict the size of the home range. Even though Fig. 3.17 shows an apparent saturation in the North-South direction, the lack of data for say, 30 days, precludes us from making any definitive conclusions regarding the home ranges using the saturation method. The lack of apparent saturation in the East-West direction also contributes to this. The Wyoming dataset was comprised of recaptures in the 1-day time-scale exclusively, so it was possible to find only diffusion constants, not home ranges, from this dataset using the saturation method. However, just for comparison purposes and without aiming at any precise results, let us extract from Fig. 3.17 the *apparent* saturation value of the mean square displacement, 1000 m^2 , using the North-South curve. Following the procedure for establishing home ranges from saturation values of the mean square displacement [3], for a grid size $G = 200 \text{ m}$ (see Fig. 3.2), assuming a box potential, we obtain a home range $L = 70 \pm 20 \text{ m}$, which is of the order of the one found in [3] ($100 \pm 25 \text{ m}$) and coincidentally similar to that found in [16] (70 m) for *Zygodontomys brevicauda* in Panama from trapping measurements in a grid arrangement.

The next natural step in future research related to this topic would be to construct a model that incorporates some of the findings in the present thesis. For instance, it is clear that diffusion constants depend on the number of individuals present at the time, thus a model where D depends explicitly on the population M , or better, on the population density u should be used. Dr. Parmenter had suggested a decaying exponential for this behavior. Even though at first sight a Gaussian shape or even a Lorentzian shape might look appropriate, considering the error involved in the diffusion constants, we can conclude that a decaying curve is appropriate to describe this behavior. The time-dependence of the diffusion constants should also be looked at in light of the results of the previous chapter. Also, dependence of D on the environmental parameter K should be considered in order to get a much better

Chapter 4. Conclusions

understanding of the situation.

In closing, we have reviewed a set of relevant topics in spatial ecology from the point of view of statistical mechanics and nonlinear science. From that perspective, we analyzed two datasets of mice motion and extracted diffusion constants, and, for comparison purposes, an estimate of a home range from the VC dataset. We hope the results presented in this thesis will be helpful to both theoretical and experimental scientists as they formulate, calibrate, and/or refine mathematical models to explain the spread of epidemics in the future.

References

- [1] R.S. Cantrell and C. Cosner, *Spatial Ecology via Reaction-Diffusion Equations*, Wiley, Chichester, West Sussex, England, 2003.
- [2] U. Dieckmann, R. Law, and J.A.J. Metz, *The Geometry of Ecological Interactions: Simplifying Spatial Complexity*, Cambridge, Cambridge, UK, 2000.
- [3] G. Abramson, L. Giuggioli, V.M. Kenkre, J.W. Dragoo, T.L. Yates, R.R. Parmenter, and C.A. Parmenter, *Diffusion and home range parameters for rodents: Peromyscus maniculatus in New Mexico*, *Ecological Complexity* **3** (2006), 64–70.
- [4] R.R. Parmenter, T.L. Yates, D.R. Anderson, K.P. Burnham, J.L. Dunnum, A.B. Franklin, M.T. Friggens, B.C. Lubow, M. Miller, G.S. Olson, C.A. Parmenter, J. Pollard, E. Rexstad, T.M. Shenk, T.R. Stanley, and G.C. White, *Small-mammal density estimation: a field comparison of grid-based vs. web-based density estimators*, *Ecological monographs* **73** (2003), 1–26.
- [5] G. Abramson and V.M. Kenkre, *Spatio-temporal Patterns in the Hantavirus Infection*, *Phys. Rev. E* **66** (2002), 011912–1–5.
- [6] V.M. Kenkre, *Results from variants of the Fisher equation in the study of epidemics and bacteria*, *Physica A* **342** (2004), 242–248.
- [7] V.M. Kenkre, *Memory Formalism, Nonlinear Techniques, and Kinetic Equation Approaches*, *Modern Challenges in Statistical Mechanics: Patterns, Noise, and the In-*

REFERENCES

- terplay of Nonlinearity and Complexity. Proceedings of the Pan American Advanced Studies Institute, Bariloche, Argentina, 2002June, pp. 63–102.
- [8] D.R. MacInnis, *Applications of Nonlinear Science and Kinetic Equations to the Spread of Epidemics*, Doctoral Dissertation, Albuquerque, NM, 2007.
- [9] D.R. MacInnis, G. Abramson, and V.M. Kenkre, *Effects of Confinement Potentials on Spatial Patterns of Infection in Hantavirus Refugia*, Preprint (2006), 1–6.
- [10] J.D. Murray, *Mathematical Biology, Second, Corrected Edition*, Springer, New York, 1993.
- [11] A. Nordsieck, W.E. Lamb, and G.E. Uhlenbeck, *On the theory of cosmic-ray showers I The furry model and the fluctuation problem*, *Physica* VII 4 (1940), 344–360.
- [12] S.H. Strogatz, *Nonlinear Dynamics and Chaos: With Applications to Physics, Biology, Chemistry, and Engineering*, Da Capo Press, Cambridge, MA, 2001.
- [13] V.M. Kenkre and M.N. Kuperman, *Applicability of the Fisher equation to bacterial population dynamics*, *Phys. Rev. E* **67** (2003), 051921–1–5.
- [14] M.G. Clerc, D. Escaff, and V.M. Kenkre, *Patterns and Localized Structures in Population Dynamics*, *Phys. Rev. E* **72** (2005), 056217–1–5.
- [15] N. Kumar, M.N. Kuperman, and V.M. Kenkre, *Theory of possible effects of the Allee phenomenon on the population of an epidemic reservoir*, *Phys. Rev. E* **79** (2009), 041902–1–6.
- [16] L. Giuggioli, G. Abramson, V.M. Kenkre, G. Suzán, E. Marcé, and T.L. Yates, *Diffusion and home range parameters from rodent population measurements in Panama*, *Bull. Math. Biol.* **67** (2005), 1135–1149.
- [17] W.H. Burt, *Territoriality and home range concepts as applied to mammals*, *J. Mammalogy* **24** (1943), 346–352.
- [18] J. Skellam, *Random dispersal in theoretical populations*, *Biometrika* **38** (1951), 196–218.

REFERENCES

- [19] H. Kierstead and L.B. Slobodkin, *The size of water masses containing plankton bloom*, J. Marine Research **12** (1953), 141–147.
- [20] W.A. Strauss, *Partial Differential Equations*, Wiley, New York, 1992.
- [21] D.G. Aronson and H.F. Weinberger, *Nonlinear diffusion in population genetics, combustion, and nerve pulse propagation*, Partial Differential Equations and Related Topics. Lecture Notes in Mathematics **446** (1975), 5–49.
- [22] D.G. Aronson and H.F. Weinberger, *Multidimensional nonlinear diffusions arising in population genetics*, Advances in Math. **30** (1978), 33–76.
- [23] D. Ludwig, D.G. Aronson, and H.F. Weinberger, *Spatial patterning of the spruce budworm*, J. Math. Biol. **8** (1979), 217–258.
- [24] M. Eigen, *Self-organization of matter and the evolution of biological macromolecules*, Naturwissenschaften **10** (1971), 465–523.
- [25] J. Maynard Smith, *Hypercycles and the origin of life*, Nature **280** (1979), 445–446.
- [26] M. Eigen and P. Schuster, *The Hypercycle: A Principle of Natural Self-organisation*, Springer, Berlin, 1979.
- [27] S.T. Nichol, C.F. Spiropoulou, S. Morzunov, P.E. Rollin, T.G. Ksiazek, H. Feldmann, A. Sanchez, J. Childs, S. Zaki, and C.J. Peters, *Genetic identification of a hantavirus associated with an outbreak of acute respiratory illness*, Science **262** (1993), 197–214.
- [28] J.E. Childs, T.G. Ksiazek, C.F. Spiropoulou, J.W. Krebs, S. Morzunov, G.O. Maupin, K.L. Gage, P.E. Rollin, J. Sarisky, R.E. Enscoe, J.K. Frey, C.J. Peters, and S.T. Nichol, *Serologic and genetic identification of *Peromyscus maniculatus* as the primary rodent reservoir for a new hantavirus in the southwestern United States*, J. Inf. Dis. **169** (1994), 1271–1280.
- [29] G. Abramson, V.M. Kenkre, T.L. Yates, and R.R. Parmenter, *Traveling waves of infection in the Hantavirus epidemic*, Bull. Math. Biol. **65** (2003), 519–534.

REFERENCES

- [30] V.M. Kenkre, *Statistical Mechanical Considerations in the Theory of the Spread of Epidemics*, Physica A **356** (2005), 121–126.
- [31] V.M. Kenkre, G. Abramson, L. Giuggioli, and G. Camelo-Neto, *Theory of Hantavirus infection spread incorporating localized adult and itinerant juvenile mice*, Eur. Phys. J. **55** (2007), 461470.
- [32] A. Okubo, *Diffusion and ecological problems: mathematical models*, Springer-Verlag, Berlin, 1979.
- [33] L.F. Stickel, *Home Range and Travels*. In: King, J.A. (editor), *Biology of Peromyscus (rodentia)*, Special Publication No. 2, The American Society of Mammalogists, Stillwater, OK **73** (1968), 373–411.
- [34] S.H. Vessey, *Long-term population trends in white-footed mice and the impact of supplemental food and shelter*, Am. Zoologist **27** (1987), 879–890.
- [35] L. Giuggioli, G. Abramson, V.M. Kenkre, R.R. Parmenter, and T.L. Yates, *Theory of home range estimation from displacement measurements of animal populations*, J. Theor. Biol. **240** (2006), 126135.
- [36] S.T. Buckland, *Distance sampling: estimating abundance of biological populations*, Chapman & Hall, London, New York, 1993.
- [37] D.R. Anderson, K.P. Burnham, G.C. White, and D.L. Otis, *Density estimation of small-mammal populations using a trapping web and distance sampling methods*, Ecology **64** (1983), 674–680.